Electronic Supplementary Information (ESI)

Hierarchical Amplification of Chirality in Anion-Coordinated Tetrahedral Cages

Jie Zhao, ‡ *[a] Mingli Lian, ‡ [b] Zijian Ni,[b] Le Yu[b] and Dong Yang*[b]

[a] School of Chemistry and Chemical Engineering, Xi'an University of Architecture and Technology, Xi'an 710055, China. E-mail: zhaojie@xauat.edu.cn

[b] Key Laboratory of Synthetic and Natural Functional Molecule of the Ministry of Education. College of Chemistry and Materials Science, Northwest University, Xi'an 710069, China. E-mail: yangdong@nwu.edu.cn

Table of Contents

S1. General considerations

All starting materials were purchased from commercial sources. 2-Nitrophenylisocyanate, (R)-(+)-1-phenylethyl isocyanate, and (S)-(-)-1-phenylethyl isocyanate were purchased from Alfa Aesar. All solvents and other reagents were of reagent grade quality and purchased commercially. All NMR spectra were recorded on a Varian unity INOVA-400, Bruker AVANCE Ⅲ HD Cryoprobe 600 MHz or Bruker AVANCE III-400 MHz spectrometer. ^{1}H and ^{13}C NMR chemical shifts were reported relative to residual solvent peaks (^{1}H NMR: 2.50 ppm for DMSO-d_6, 1.94 ppm for CD_3CN respectively; ^{13}C NMR: 39.52 for DMSO-d_6). High resolution mass spectra (HRMS) were performed with a Bruker micrOTOF-Q II (Germany). Circular Dichroism (CD) spectra were recorded on a J-1500 spectropolarimeter (Jasco, Japan).

S2. Synthesis and characterization

S2.1 Synthesis of ligand L$^{R/S}$

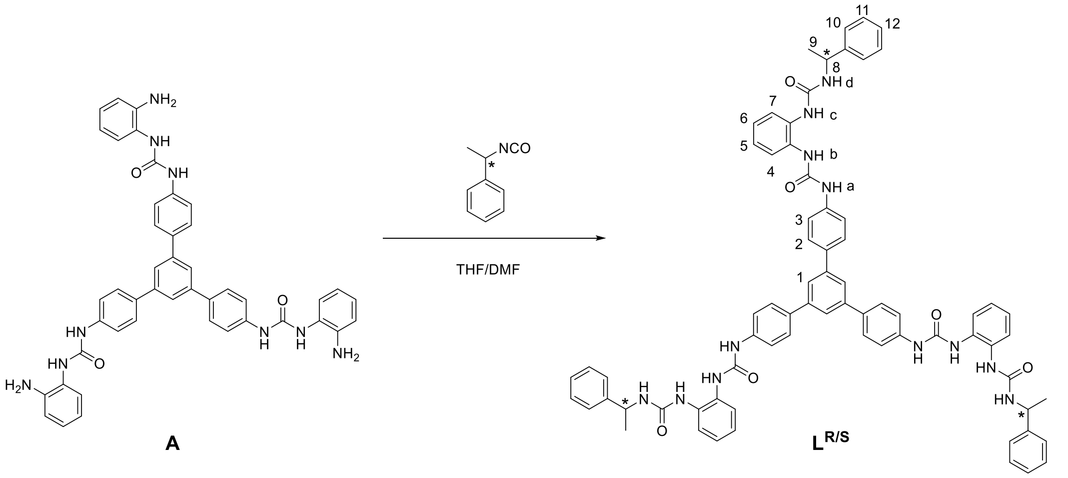

Scheme S1. Synthesis of ligands **L$^{R/S}$**.

Compound A

Compound **A** was synthesized according to literature procedures.[1]

Ligand L^{R}

(R)-(+)-1-phenylethyl isocyanate (160 μL, 1.13 mmol) was dissolved in 15 mL THF and then added to a DMF solution (5 mL) of compound **A** (200 mg, 0.27 mmol). After stirring overnight at 85 ºC, the precipitate was filtered off, washed with diethyl ether and then dried over in vacuum to yield **L^{R}** as a white solid (216.7 mg, 80 %). ^{1}H NMR (400 MHz, DMSO-d_6, ppm): δ 9.19 (s, 1H, NHd), 8.01 (s, 1H, NHc), 7.88 (s, 1H, NHb), 7.81 (s, 1H, NHa), 7.80 (d, 2H, H3), 7.61 (d, 3H, H1/H4/H7), 7.48 (d, 1H, H10), 7.35 (m, 4H, H2/H11), 7.23 (m, 1H, H10), 7.06 (m,3H, H5/H6/H12), 4.86 (s, 1H, H8), 1.40 (d, 3H, H9). ^{13}C NMR (100 MHz, DMSO-d_6, ppm): δ 155.5, 153.9, 145.7, 141.7, 140.3, 134.0, 133.5, 130.2, 128.9, 127.9, 127.2, 126.5, 125.5, 124.9, 123.4, 123.1, 123.0, 118.9, 49.4, 23.6.

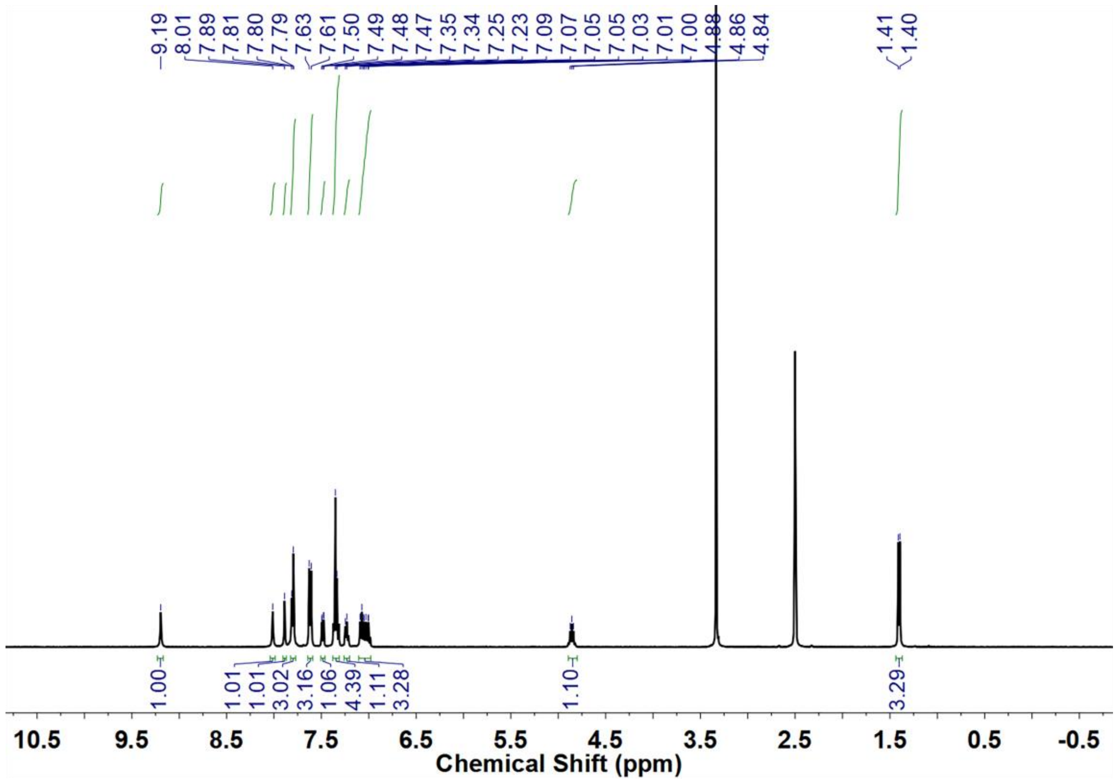

Figure S1. ^{1}H NMR spectrum (400 MHz, DMSO-d_6, 298 K) of $\mathbf{L^R}$.

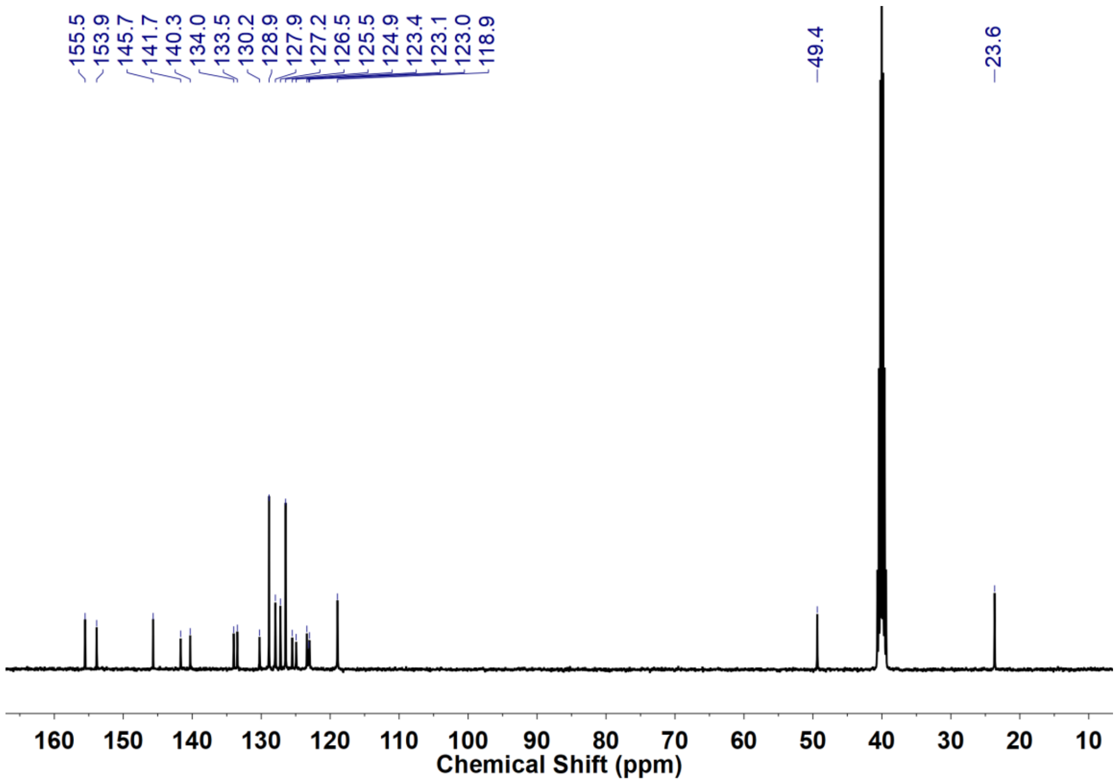

Figure S2. ^{13}C NMR spectrum (100 MHz, DMSO-d_6, 298 K) of $\mathbf{L^R}$.

Ligand L^S

(S)-(-)-1-phenylethyl isocyanate (160 μL, 1.13 mmol) was dissolved in 15 mL THF and then added to a DMF solution (5 mL) of compound **A** (200 mg, 0.27 mmol). After stirring overnight at 85 ºC, the precipitate was filtered off, washed with diethyl ether and then dried over in vacuum to yield $\mathbf{L^S}$ as a white solid (191.5 mg, 71%). ^{1}H NMR (400 MHz, DMSO-d_6, ppm): δ 9.20 (s, 1H, NHd), 8.01 (s, 1H, NHc), 7.88 (s, 1H, NHb), 7.81 (s, 1H, NHa), 7.80 (d, 2H, H3), 7.61 (d, 3H, H1/H4/H7), 7.48 (d, 1H, H10), 7.35 (m, 4H, H2/H11), 7.23 (m, 1H, H10), 7.06 (m,3H, H5/H6/H12), 4.86 (s, 1H, H8), 1.40 (d, 3H, H9). ^{13}C NMR (100 MHz, DMSO-d_6, ppm): δ 155.5, 153.9, 145.7, 141.7, 140.3, 134.0, 133.5, 130.2, 128.9, 127.9, 127.2, 126.5, 125.5, 124.9, 123.4, 123.1, 123.0, 118.9, 49.4, 23.6.

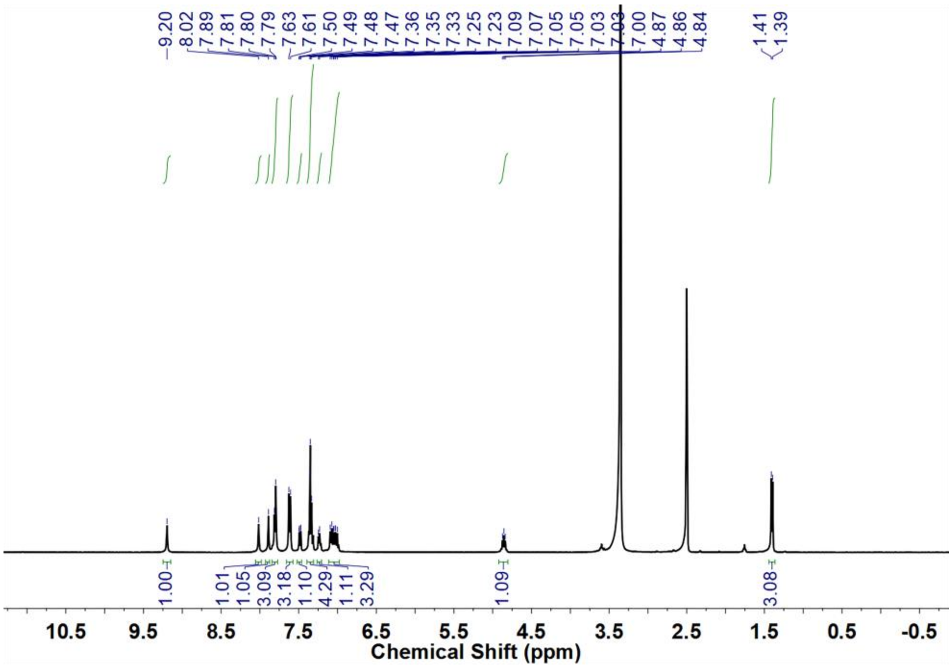

Figure S3. ^{1}H NMR spectrum (400 MHz, DMSO-d_6, 298 K) of $\mathbf{L^S}$.

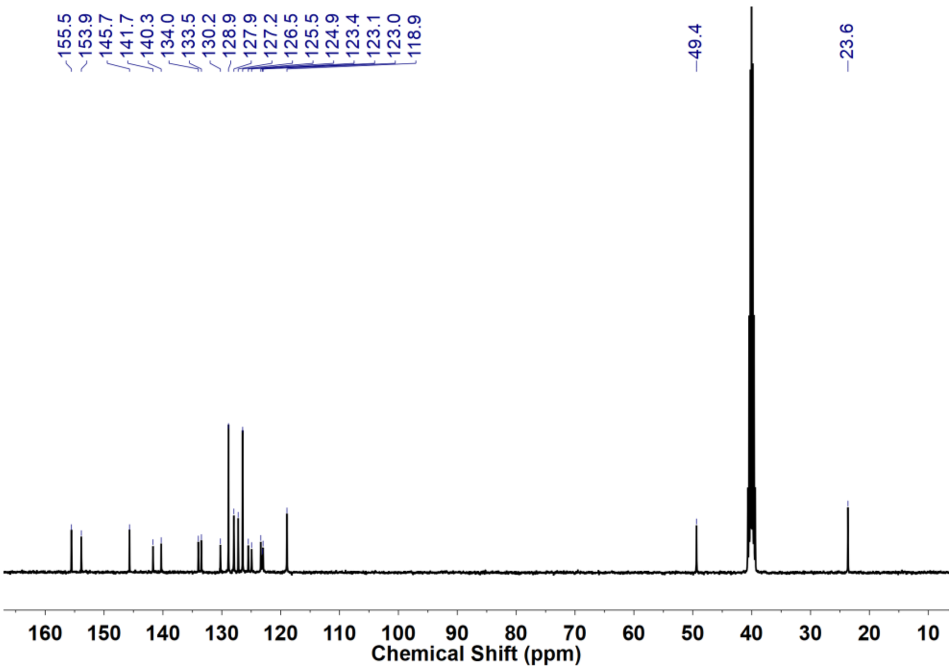

Figure S4. ^{13}C NMR spectrum (100 MHz, DMSO-d_6, 298 K) of $\mathbf{L^S}$.

S2.2 Synthesis of $1^{R/S}$ and $2^{R/S}$

$[K(18\text{-}C\text{-}6)]_3PO_4$ or $[K(18\text{-}C\text{-}6)]_2CO_3$ (generated in situ from 18-Crown-6 and K_3PO_4 or K_2CO_3) (8.0 μL, 5 μmol) was added to a suspension of $\mathbf{L}^{R/S}$ (5.96 mg) in acetonitrile (1 mL). After stirring overnight at room temperature, a clear light brown solution was obtained. The corresponding "aniono" complexes $\mathbf{1}^{R/S}$ and $\mathbf{2}^{R/S}$ were then obtained by precipitate with adding diethyl ether into the above solution.

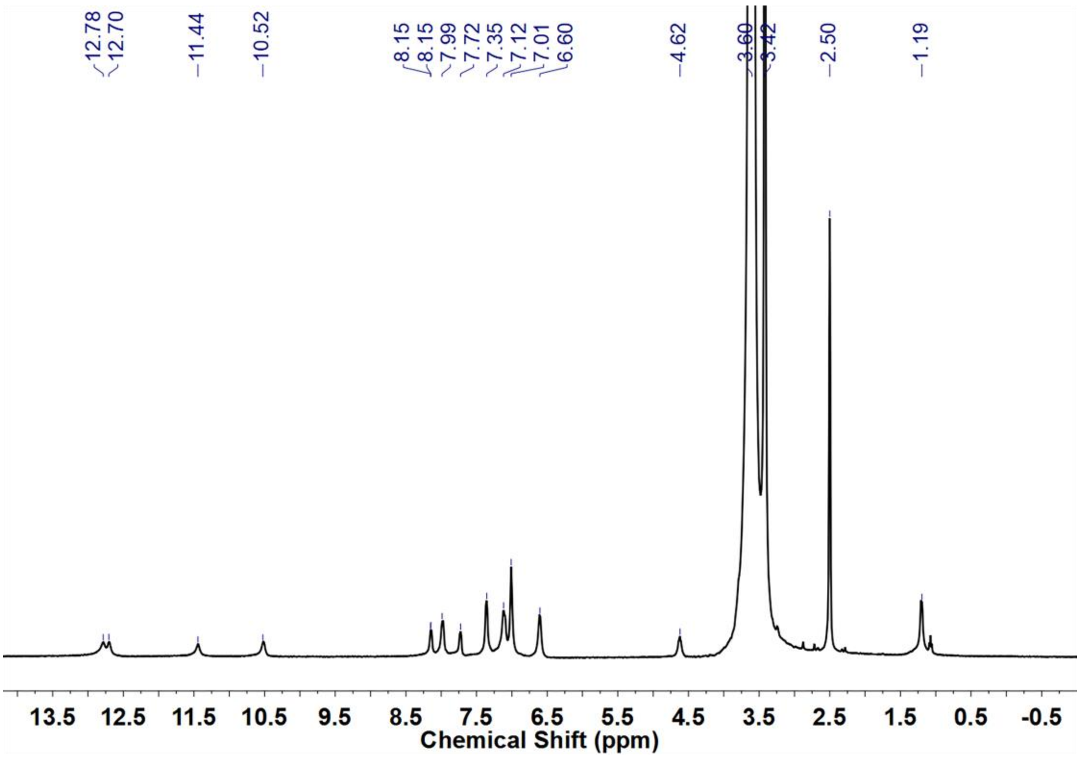

Figure S5. ^{1}H NMR spectrum (400 MHz, DMSO-d_6, 298 K) of $\mathbf{1}^{R}$.

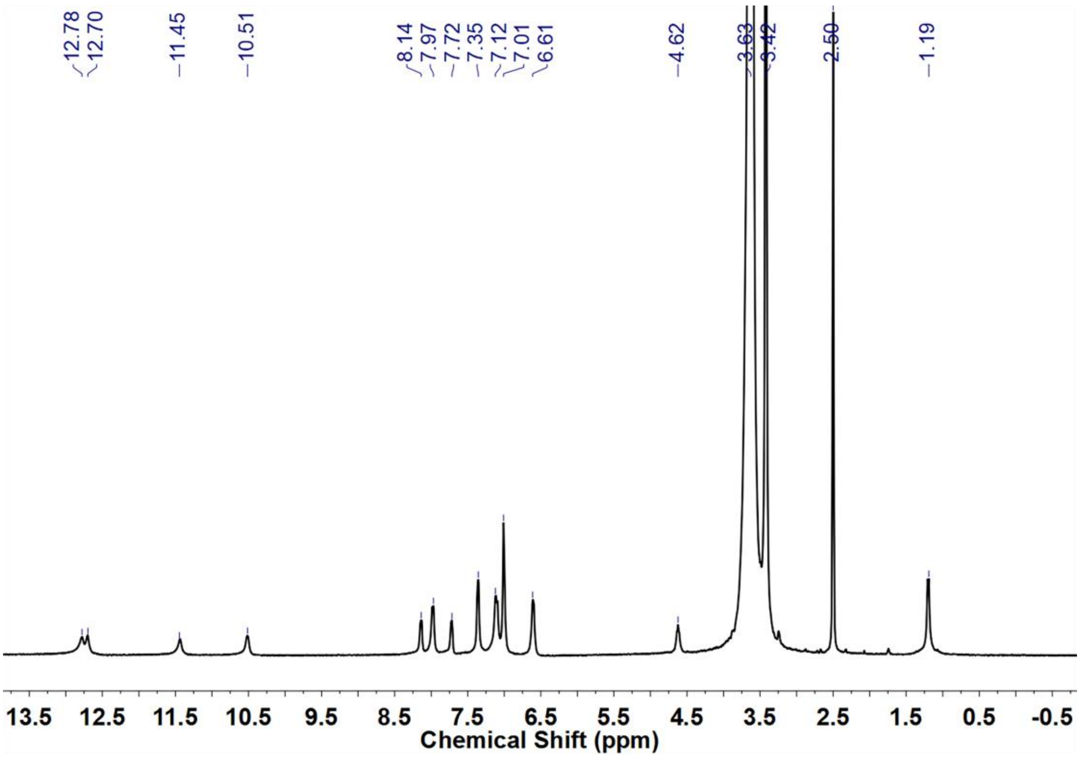

Figure S6. ^{1}H NMR spectrum (400 MHz, DMSO-d_6, 298 K) of $\mathbf{1}^{S}$.

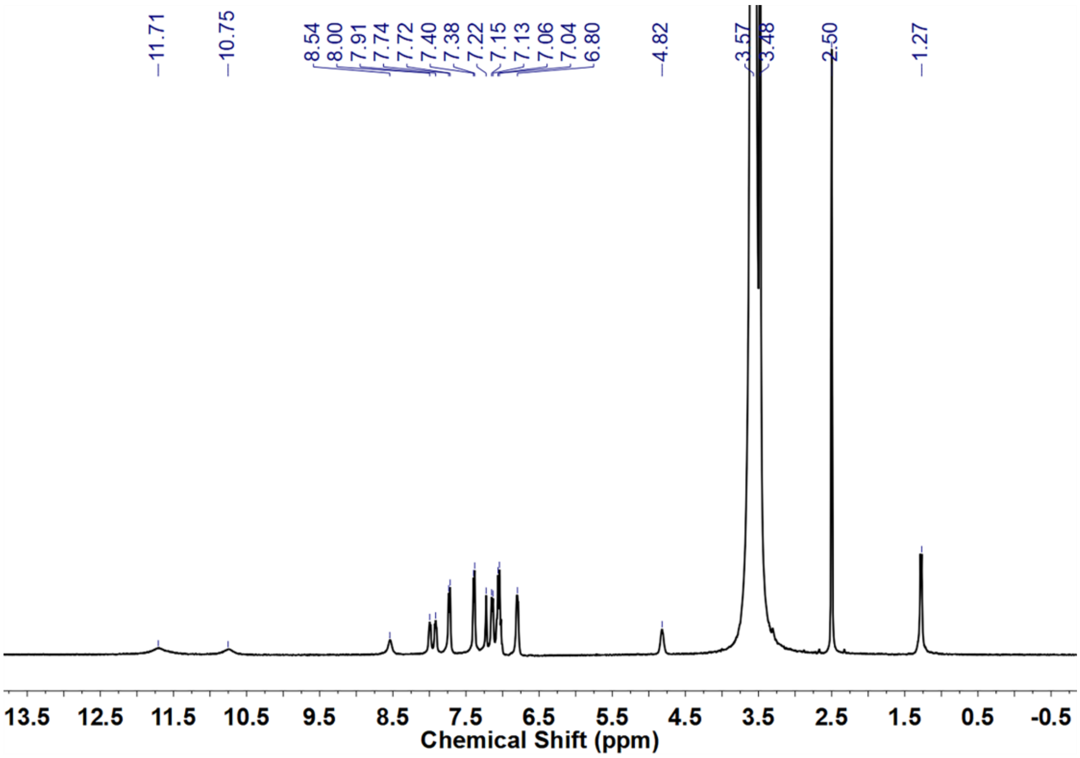

Figure S7. ^{1}H NMR spectrum (400 MHz, DMSO-d_6, 298 K) of $\mathbf{2^R}$.

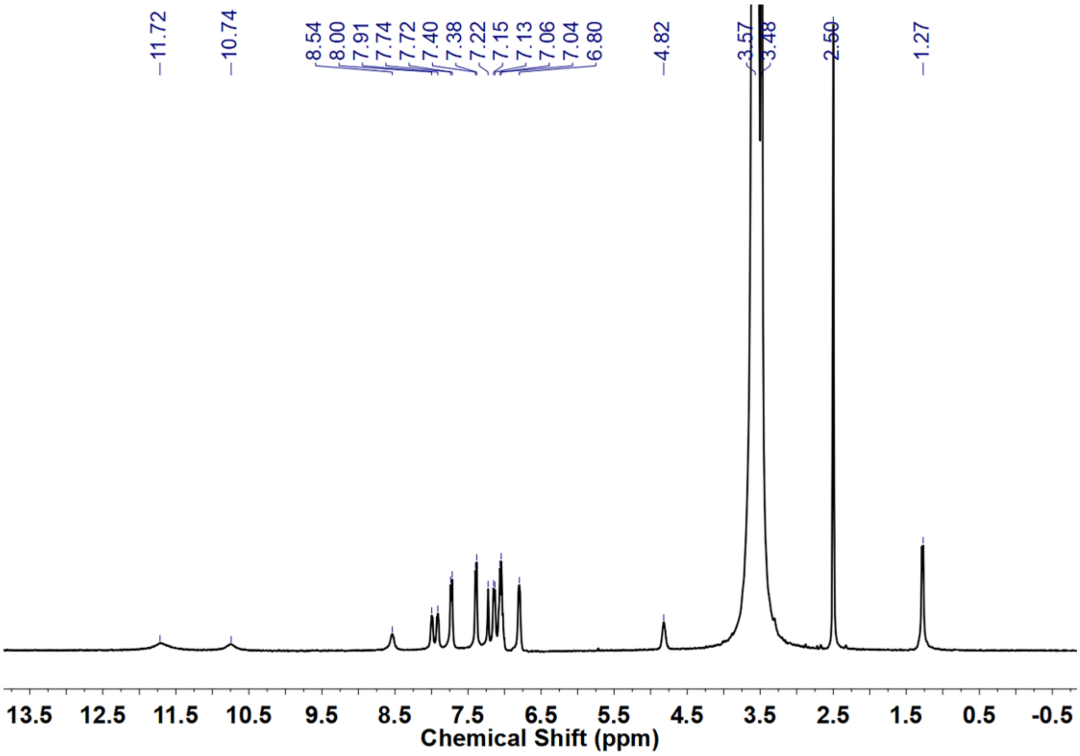

Figure S8. ^{1}H NMR spectrum (400 MHz, DMSO-d_6, 298 K) of $\mathbf{2^S}$.

Table S1. The chemical shifts of NH signals of urea groups in $\mathbf{1}^{R/S}$ and $\mathbf{2}^{R/S}$.

	Ha	Hb	Hc	Hd
$\mathbf{1}^{R}$	2.71	3.55	4.68	3.58
$\mathbf{1}^{S}$	2.70	3.56	4.68	3.58
$\mathbf{2}^{R}$	0.73	2.86	3.69	2.51
$\mathbf{2}^{S}$	0.73	2.85	3.70	2.52

S2.3 Synthesis of $(TMA)_6(CO_3)_3(L^S)_2$ ($\mathbf{2}^S$) and $(TMA)_8(CO_3)_4(L^S)_4$ ($\mathbf{3}^S \supset TMA^+$)

$(TMA)_2CO_3$ (12.0 µL, 7.5 µmol) was added to a suspension of $\mathbf{L}^S$ (5.96 mg) in DMSO (0.5 mL). After stirring overnight at room temperature, a clear light brown solution was obtained. The corresponding "aniono" complexes $\mathbf{2}^S$ were obtained. ^{13}C NMR (100 MHz, DMSO-d_6, ppm): δ 164.1, 155.4, 146.7, 142.4, 141.5, 131.5, 128.1, 126.8, 126.2, 126.1, 121.6, 120.8, 120.3, 119.5, 119.0, 65.0, 54.5, 48.8, 23.4, 15.2. Anal. Calcd for $C_{171}H_{204}N_{30}O_{21}$: C, 68.1%; H, 6.8%; N, 13.9%. Found: C, 71.0%; H, 6.9%; N, 13.7%.

$(TMA)_2CO_3$ (6.4 µL, 4 µmol) was added to a suspension of $\mathbf{L}^S$ (4.78 mg) in acetonitrile (1 mL). After stirring overnight at room temperature, a clear light brown solution was obtained. The corresponding "aniono" complexes $\mathbf{3}^S \supset TMA^+$ were obtained. ^{13}C NMR (150 MHz, acetonitrile-d_3, ppm): δ 156.4, 154.9, 147.3, 141.9, 141.6, 132.3, 131.6, 129.1, 128.6, 127.2, 126.9, 126.5, 123.7, 123.6, 122.0, 121.3, 120.8, 120.3, 118.3, 55.9, 53.9, 49.9, 23.2. Anal. Calcd for $C_{324}H_{360}N_{56}O_{36}$: C, 69.3%; H, 6.5%; N, 14.0%. Found: C, 73.2%; H, 6.6%; N, 13.9%.

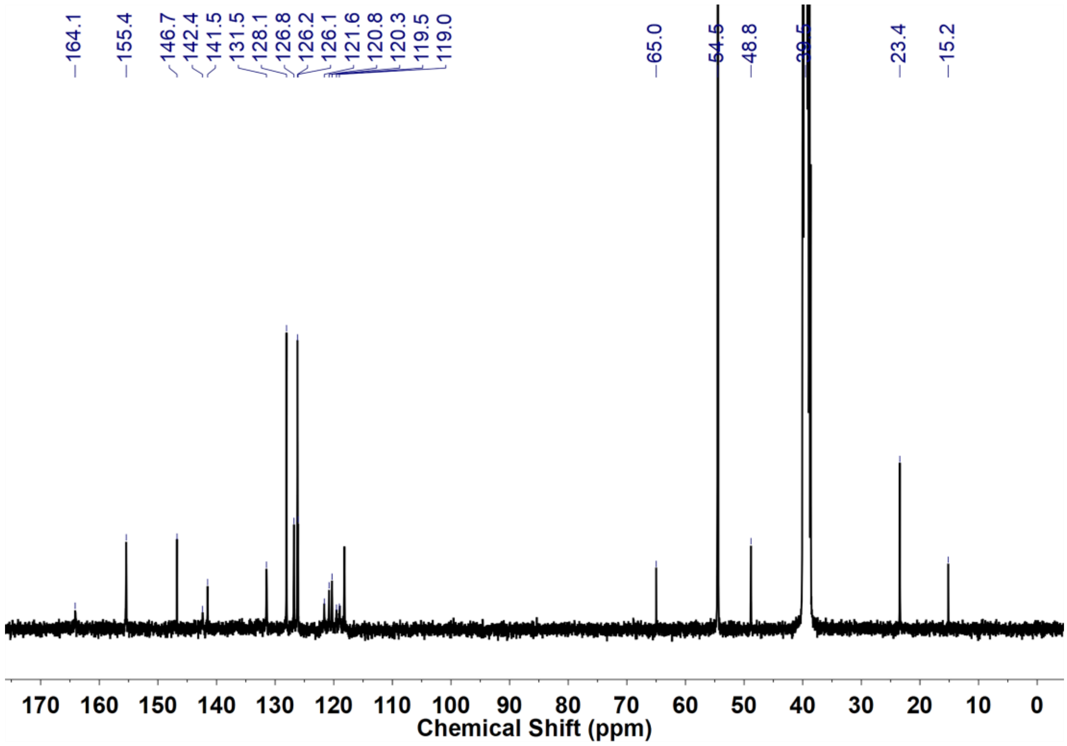

Figure S9. ^{13}C NMR spectrum (100 MHz, DMSO-d_6, 298 K) of $(CO_3)_3\mathbf{L}^S{}_2$ (generated from $\mathbf{L}^S$ and $(TMA)_2CO_3$).

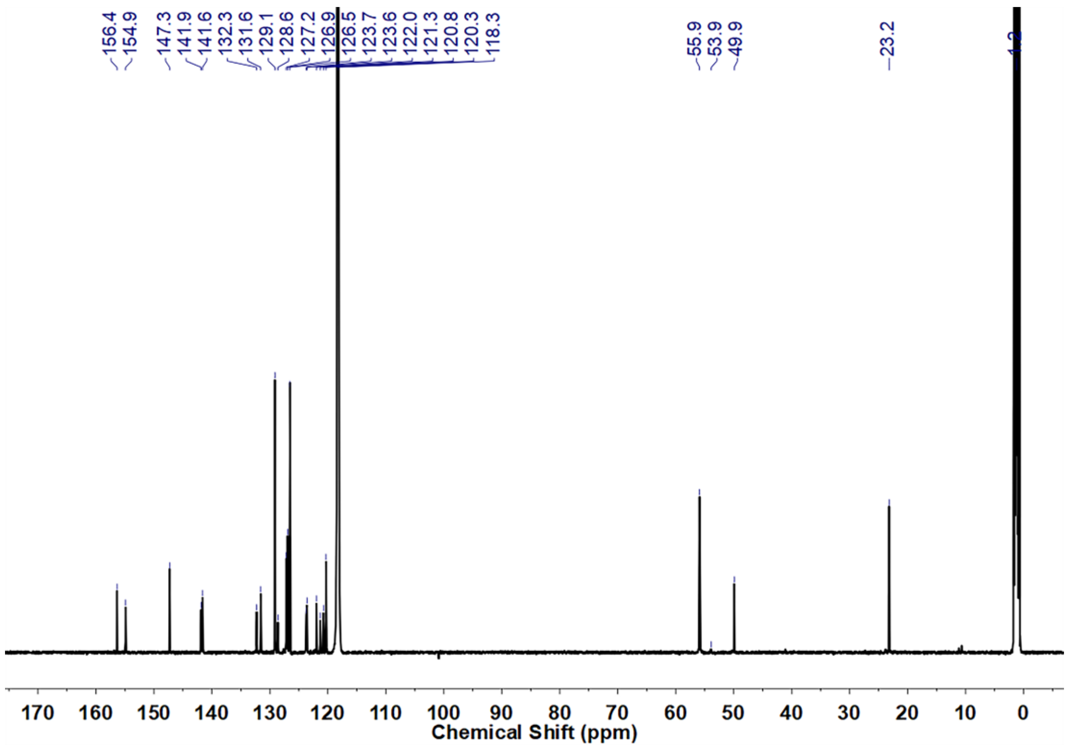

Figure S10. [13]C NMR spectrum (150 MHz, acetonitrile-d_3, 298 K) of $(CO_3)_4$**L**$^S{}_4$ (generated from **L**^{S} and $(TMA)_2CO_3$).

S3. High-resolution ESI-MS spectra

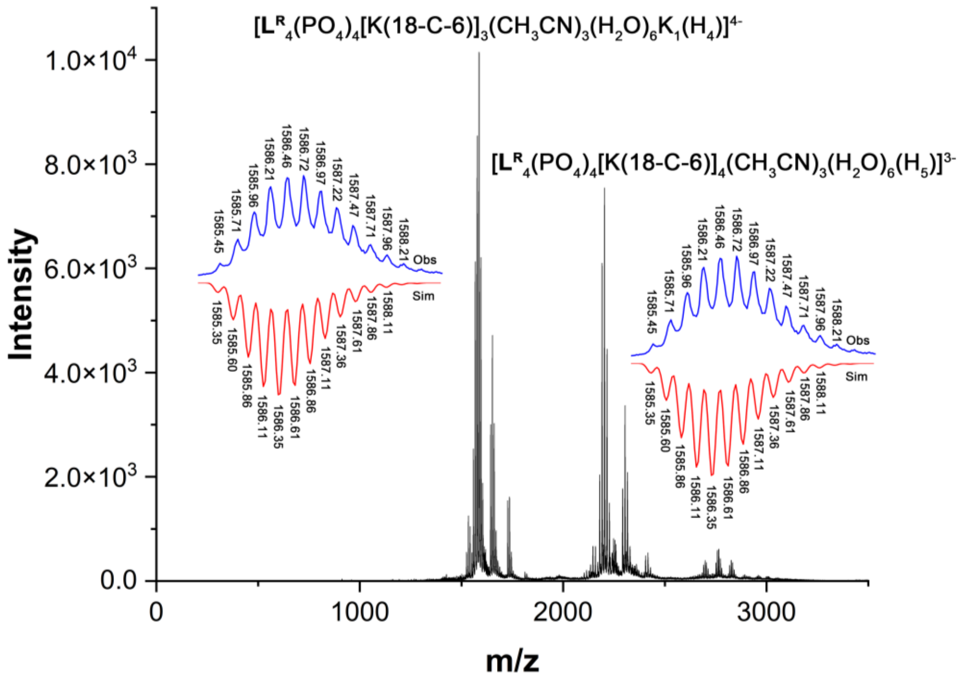

Figure S11. HR ESI-mass spectrum of **1**^{R} in CH_3CN.

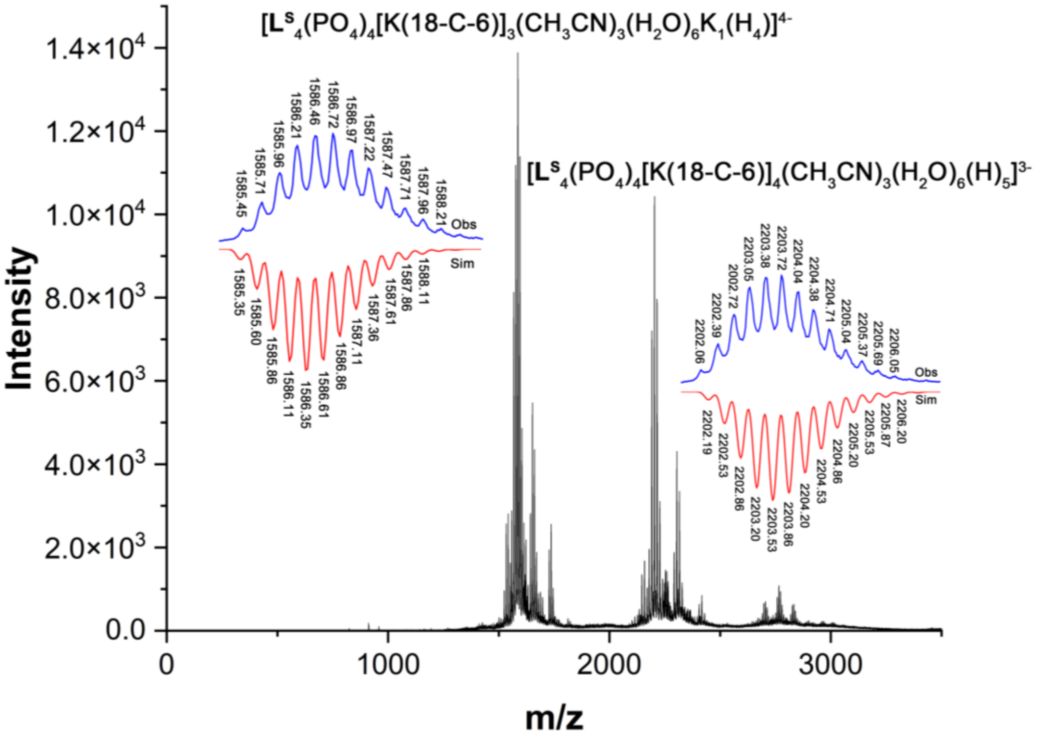

Figure S12. HR ESI-mass spectrum of $\mathbf{1^S}$ in CH_3CN.

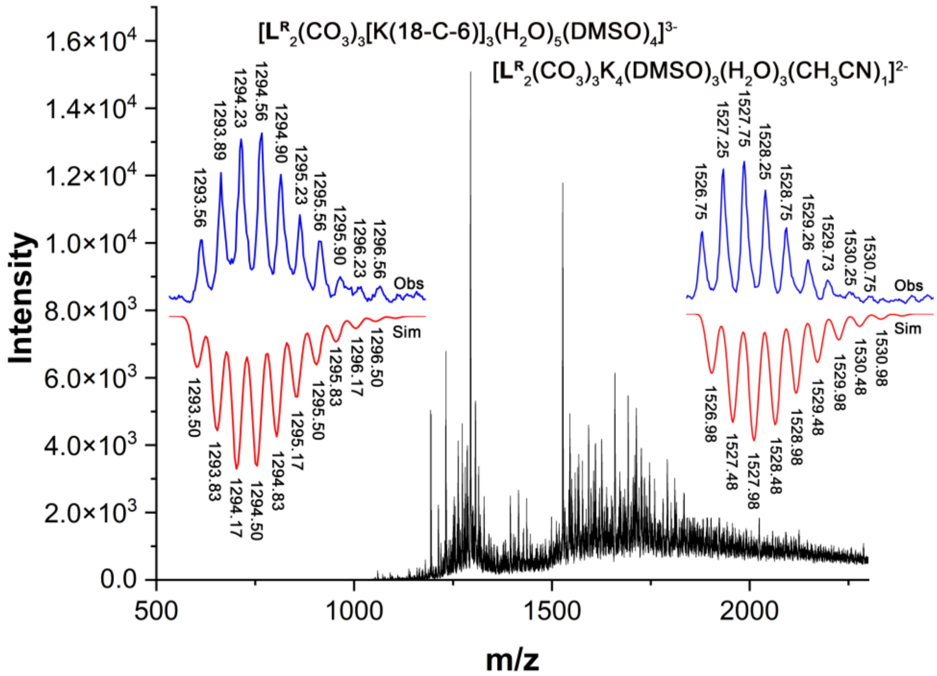

Figure S13. HR ESI-mass spectrum of $\mathbf{2^R}$ in DMSO.

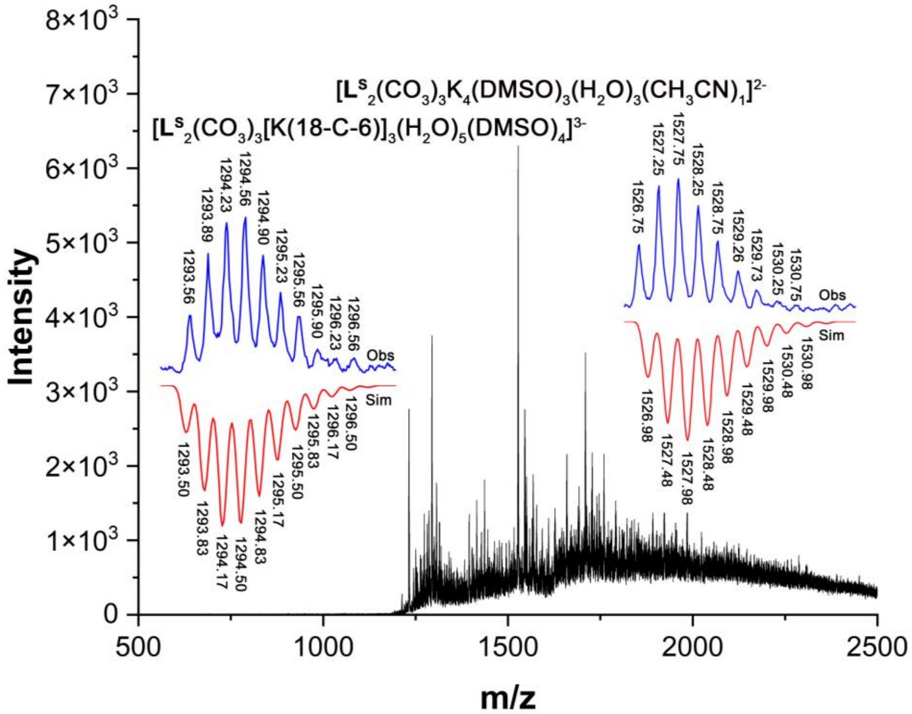

Figure S14. HR ESI-mass spectrum of $\mathbf{2^S}$ in DMSO.

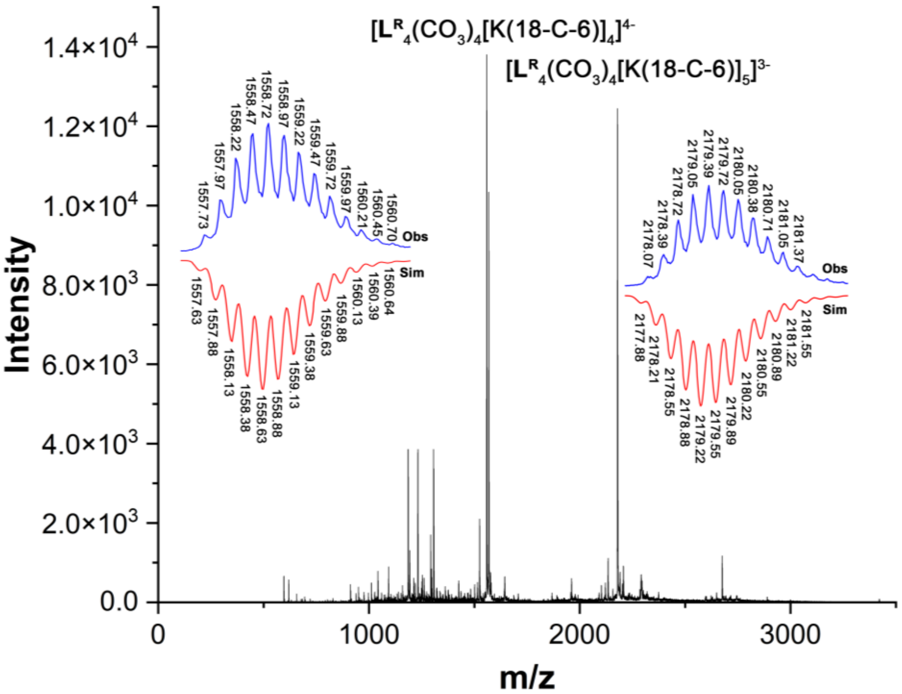

Figure S15. HR ESI-mass spectrum of $\mathbf{3^R}$ in CH_3CN.

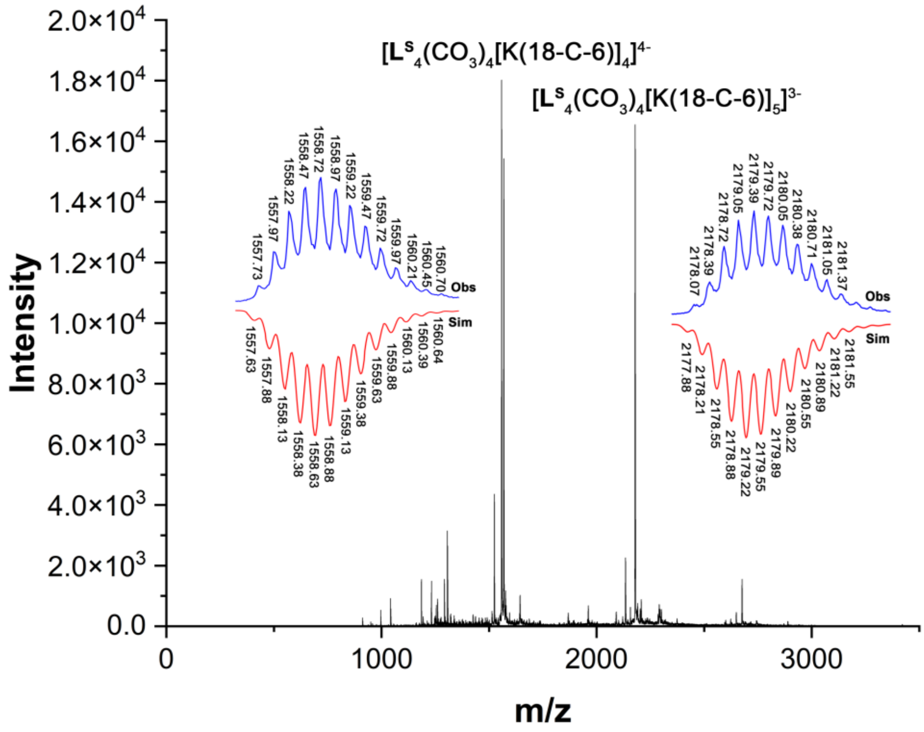

Figure S16. HR ESI-mass spectrum of $\mathbf{3^S}$ in CH_3CN.

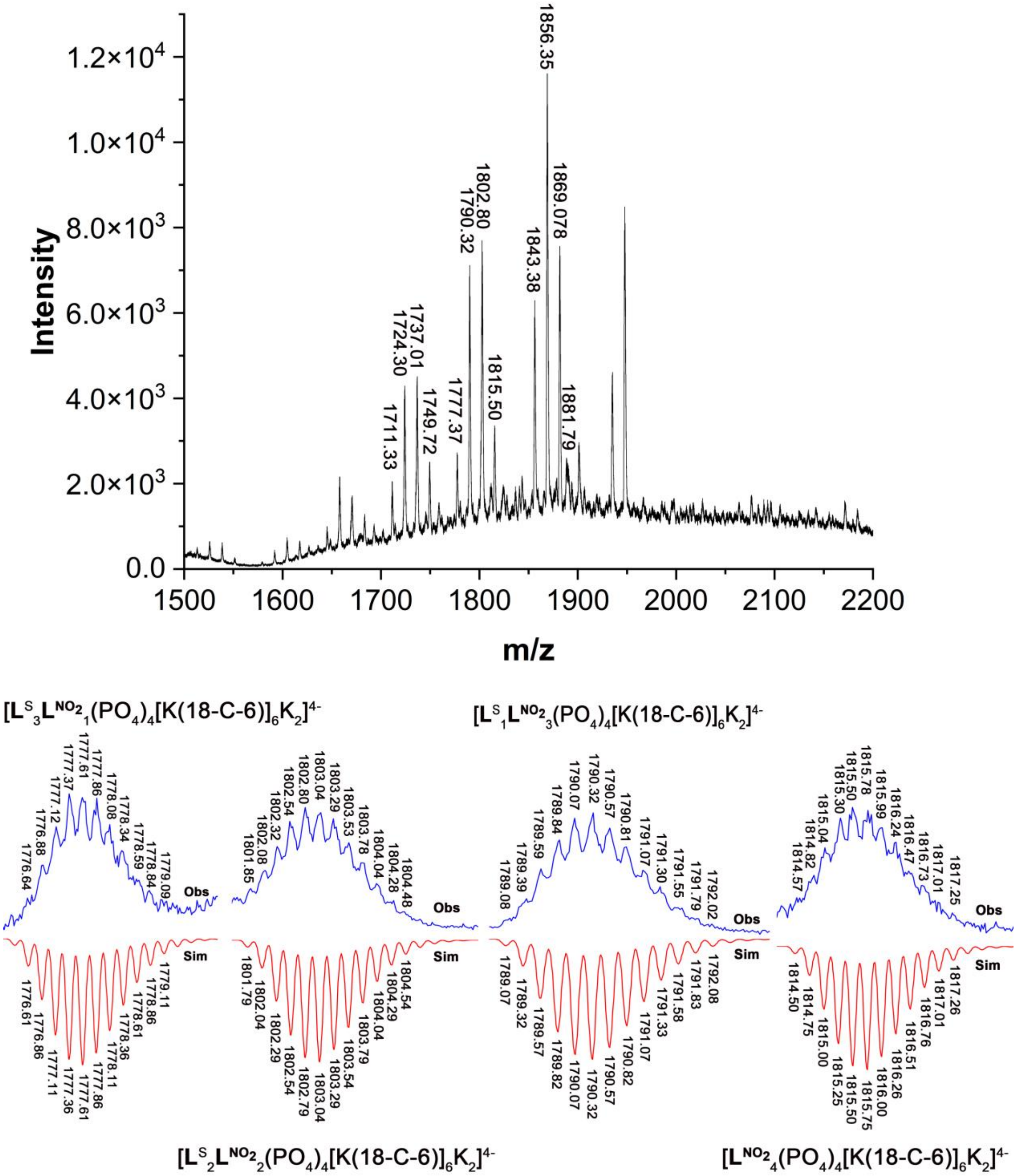

Figure S17. HR ESI-mass spectrum of phosphate-coordinated mixed-ligand cages (**L**^{S} : **L**^{NO2} = 1 : 3) in a mixed solvent of CH_3CN and DMSO (volume ratio of 9 : 1).

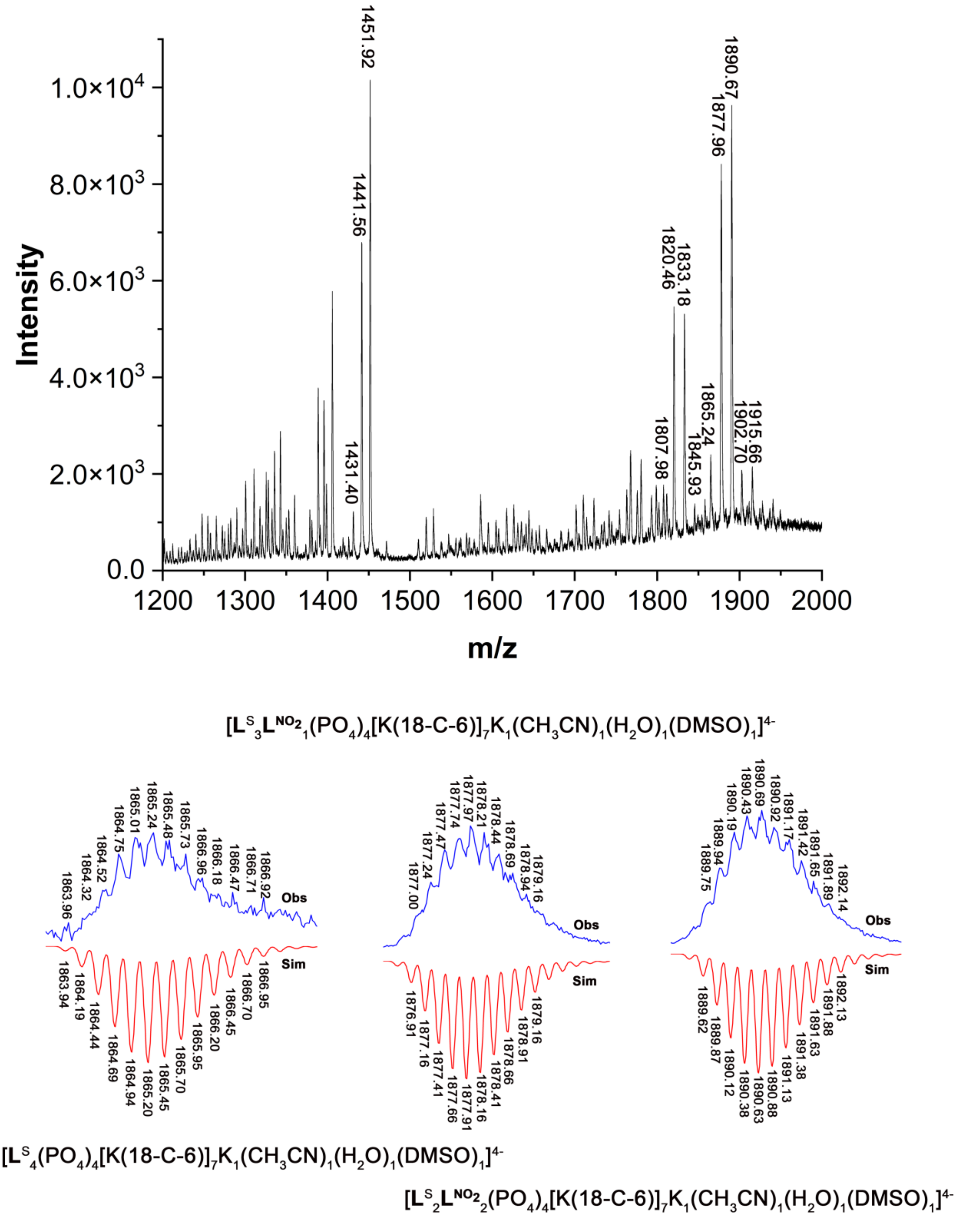

Figure S18. HR ESI-mass spectrum of phosphate-coordinated mixed-ligand cages (**L**^{S} : **L**^{NO2} = 1 : 3) with addition of TMA^{+} in a mixed solvent of CH_3CN and DMSO (volume ratio of 9 : 1).

Table S2. The summary of HR ESI-MS data of the phosphate-coordinated mixed-ligand cages ($\mathbf{L}^{S}$: $\mathbf{L}^{NO_2}$ = 1 : 3) in a mixed solvent of CH_3CN and DMSO (volume ratio of 9 : 1).

m/z	*z*	**Formula**
1711.33	-4	$[\mathbf{L}^{S}{}_3\mathbf{L}^{NO_2}{}_1(PO_4)_4[K(18\text{-}C\text{-}6)]_5K_3]^{4-}$
1724.30	-4	$[\mathbf{L}^{S}{}_2\mathbf{L}^{NO_2}{}_2(PO_4)_4[K(18\text{-}C\text{-}6)]_5K_3]^{4-}$
1737.01	-4	$[\mathbf{L}^{S}{}_1\mathbf{L}^{NO_2}{}_3(PO_4)_4[K(18\text{-}C\text{-}6)]_5K_3]^{4-}$
1749.72	-4	$[\mathbf{L}^{NO_2}{}_4(PO_4)_4[K(18\text{-}C\text{-}6)]_5K_3]^{4-}$
1777.37	-4	$[\mathbf{L}^{S}{}_3\mathbf{L}^{NO_2}{}_1(PO_4)_4[K(18\text{-}C\text{-}6)]_6K_2]^{4-}$
1790.32	-4	$[\mathbf{L}^{S}{}_2\mathbf{L}^{NO_2}{}_2(PO_4)_4[K(18\text{-}C\text{-}6)]_6K_2]^{4-}$
1802.80	-4	$[\mathbf{L}^{S}{}_1\mathbf{L}^{NO_2}{}_3(PO_4)_4[K(18\text{-}C\text{-}6)]_6K_2]^{4-}$
1815.50	-4	$[\mathbf{L}^{NO_2}{}_4(PO_4)_4[K(18\text{-}C\text{-}6)]_6K_2]^{4-}$
1843.38	-4	$[\mathbf{L}^{S}{}_3\mathbf{L}^{NO_2}{}_1(PO_4)_4[K(18\text{-}C\text{-}6)]_7K_1]^{4-}$
1856.35	-4	$[\mathbf{L}^{S}{}_2\mathbf{L}^{NO_2}{}_2(PO_4)_4[K(18\text{-}C\text{-}6)]_7K_1]^{4-}$
1869.07	-4	$[\mathbf{L}^{S}{}_1\mathbf{L}^{NO_2}{}_3(PO_4)_4[K(18\text{-}C\text{-}6)]_7K_1]^{4-}$
1881.79	-4	$[\mathbf{L}^{NO_2}{}_4(PO_4)_4[K(18\text{-}C\text{-}6)]_7K_1]^{4-}$

Table S3. The summary of HR ESI-MS data of the phosphate-coordinated mixed-ligand cages ($\mathbf{L}^{S}$: $\mathbf{L}^{NO_2}$ = 1 : 3) with addition of TMA^+ in a mixed solvent of CH_3CN and DMSO (volume ratio of 9 : 1).

m/z	*z*	**Formula**
1431.40	-5	$[\mathbf{L}^{S}{}_4(PO_4)_4[K(18\text{-}C\text{-}6)]_6K_1(H_2O)_1(CH_3CN)_1(DMSO)_1]^{5-}$
1441.56	-5	$[\mathbf{L}^{S}{}_3\mathbf{L}^{NO_2}{}_1(PO_4)_4[K(18\text{-}C\text{-}6)]_6K_1(H_2O)_1(CH_3CN)_1(DMSO)_1]^{5-}$
1451.92	-5	$[\mathbf{L}^{S}{}_2\mathbf{L}^{NO_2}{}_2(PO_4)_4[K(18\text{-}C\text{-}6)]_6K_1(H_2O)_1(CH_3CN)_1(DMSO)_1]^{5-}$
1807.98	-4	$[\mathbf{L}^{S}{}_4(PO_4)_4[K(18\text{-}C\text{-}6)]_6K_2(H_2O)_1(CH_3CN)_1(DMSO)_1(CH_3OH)_1]^{4-}$
1820.46	-4	$[\mathbf{L}^{S}{}_3\mathbf{L}^{NO_2}{}_1(PO_4)_4[K(18\text{-}C\text{-}6)]_6K_2(H_2O)_1(CH_3CN)_1(DMSO)_1(CH_3OH)_1]^{4-}$
1833.18	-4	$[\mathbf{L}^{S}{}_2\mathbf{L}^{NO_2}{}_2(PO_4)_4[K(18\text{-}C\text{-}6)]_6K_2(H_2O)_1(CH_3CN)_1(DMSO)_1(CH_3OH)_1]^{4-}$
1845.93	-4	$[\mathbf{L}^{S}{}_1\mathbf{L}^{NO_2}{}_3(PO_4)_4[K(18\text{-}C\text{-}6)]_6K_2(H_2O)_1(CH_3CN)_1(DMSO)_1(CH_3OH)_1]^{4-}$
1865.24	-4	$[\mathbf{L}^{S}{}_4(PO_4)_4[K(18\text{-}C\text{-}6)]_7K_1(H_2O)_1(CH_3CN)_1(DMSO)_1]^{4-}$

1877.96	-4	$[\mathbf{L}^{S}_{3}\mathbf{L}^{NO_2}{}_{1}(PO_4)_4[K(18\text{-}C\text{-}6)]_7K_1(H_2O)_1(CH_3CN)_1(DMSO)_1]^{4-}$
1890.67	-4	$[\mathbf{L}^{S}_{2}\mathbf{L}^{NO_2}{}_{2}(PO_4)_4[K(18\text{-}C\text{-}6)]_7K_1(H_2O)_1(CH_3CN)_1(DMSO)_1]^{4-}$
1902.70	-4	$[\mathbf{L}^{S}_{1}\mathbf{L}^{NO_2}{}_{3}(PO_4)_4[K(18\text{-}C\text{-}6)]_7K_1(H_2O)_1(CH_3CN)_1(DMSO)_1]^{4-}$
1915.66	-4	$[\mathbf{L}^{NO_2}{}_{4}(PO_4)_4[K(18\text{-}C\text{-}6)]_7K_1(H_2O)_1(CH_3CN)_1(DMSO)_1]^{4-}$

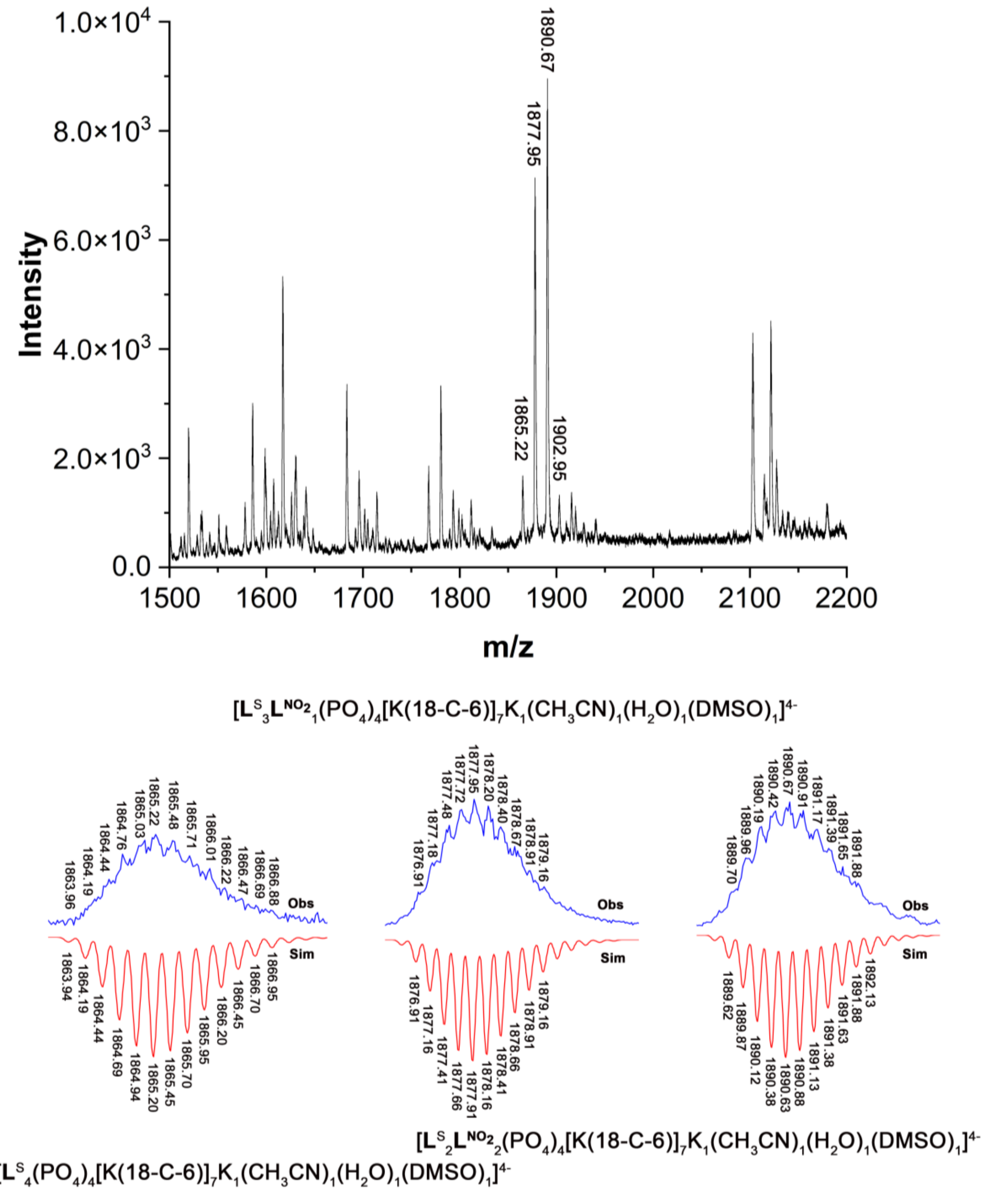

Figure S19. HR ESI-mass spectrum of phosphate-coordinated mixed-ligand cages ($\mathbf{L}^{S}$: $\mathbf{L}^{NO_2}$ = 1 : 1) in a mixed solvent of CH_3CN and DMSO (volume ratio of 9 : 1).

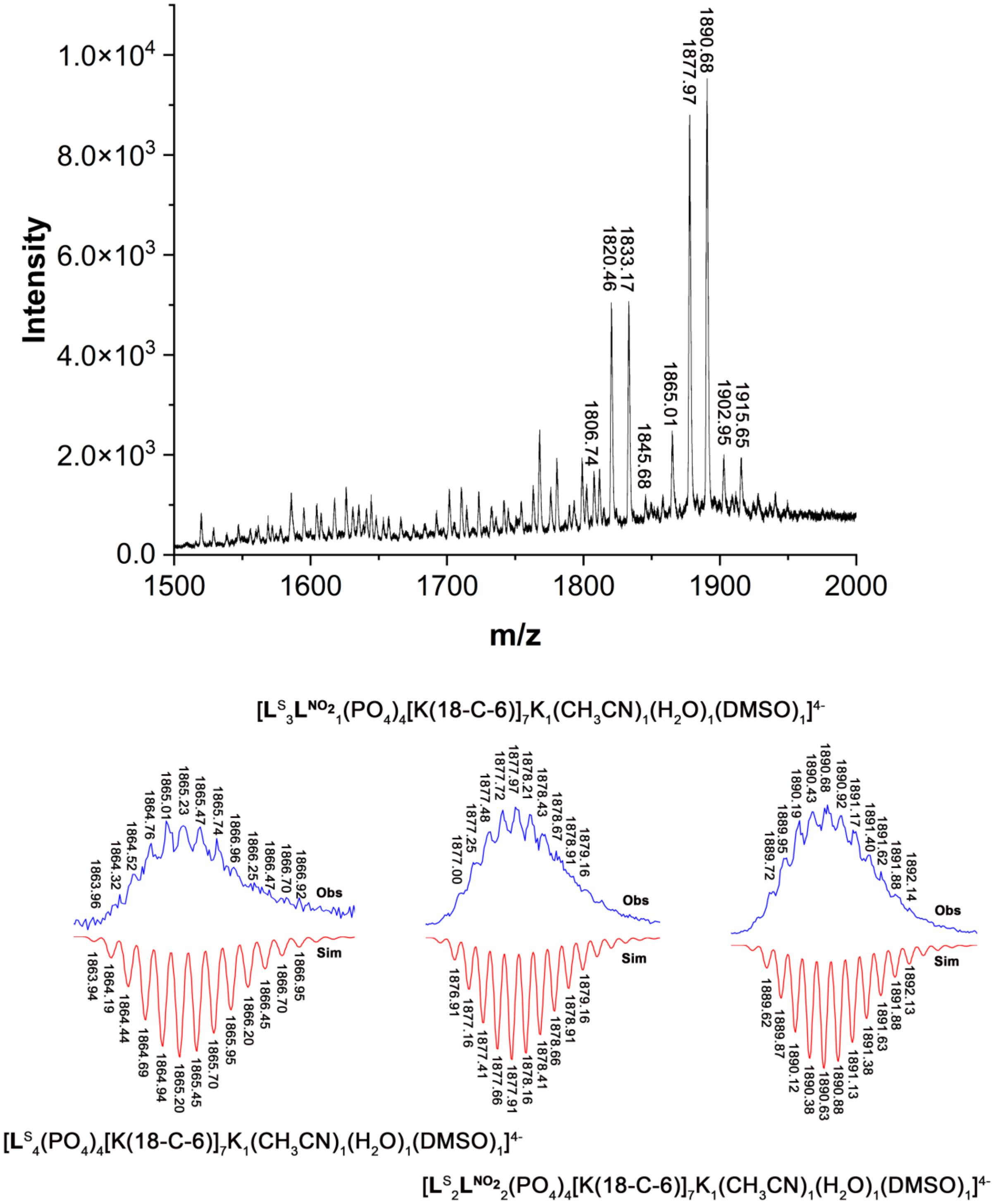

Figure S20. HR ESI-mass spectrum of phosphate-coordinated mixed-ligand cages (**L**^{S} : **L**^{NO2} = 1 : 1) with addition of TMA^{+} in a mixed solvent of CH_3CN and DMSO (volume ratio of 9 : 1).

Table S4. The summary of HR ESI-MS data of the phosphate-coordinated mixed-ligand cages ($\mathbf{L}^{\mathbf{S}}$: $\mathbf{L}^{\mathbf{NO2}}$ = 1 : 1) in a mixed solvent of CH_3CN and DMSO (volume ratio of 9 : 1).

m/z	*z*	**Formula**
1865.22	-4	$[\mathbf{L}^{\mathbf{S}}{}_4(PO_4)_4[K(18\text{-}C\text{-}6)]_7K_1(H_2O)_1(CH_3CN)_1(DMSO)_1]^{4-}$
1877.95	-4	$[\mathbf{L}^{\mathbf{S}}{}_3\mathbf{L}^{\mathbf{NO2}}{}_1(PO_4)_4[K(18\text{-}C\text{-}6)]_7K_1(H_2O)_1(CH_3CN)_1(DMSO)_1]^{4-}$
1890.67	-4	$[\mathbf{L}^{\mathbf{S}}{}_2\mathbf{L}^{\mathbf{NO2}}{}_2(PO_4)_4[K(18\text{-}C\text{-}6)]_7K_1(H_2O)_1(CH_3CN)_1(DMSO)_1]^{4-}$
1902.95	-4	$[\mathbf{L}^{\mathbf{S}}{}_1\mathbf{L}^{\mathbf{NO2}}{}_3(PO_4)_4[K(18\text{-}C\text{-}6)]_7K_1(H_2O)_1(CH_3CN)_1(DMSO)_1]^{4-}$

Table S5. The summary of HR ESI-MS data of the phosphate-coordinated mixed-ligand cages ($\mathbf{L}^{\mathbf{S}}$: $\mathbf{L}^{\mathbf{NO2}}$ = 1 : 1) with addition of TMA^+ in a mixed solvent of CH_3CN and DMSO (volume ratio of 9 : 1).

m/z	*z*	**Formula**
1806.74	-4	$[\mathbf{L}^{\mathbf{S}}{}_4(PO_4)_4[K(18\text{-}C\text{-}6)]_6K_2(H_2O)_1(CH_3CN)_1(DMSO)_1(CH_3OH)_1]^{4-}$
1820.46	-4	$[\mathbf{L}^{\mathbf{S}}{}_3\mathbf{L}^{\mathbf{NO2}}{}_1(PO_4)_4[K(18\text{-}C\text{-}6)]_6K_2(H_2O)_1(CH_3CN)_1(DMSO)_1(CH_3OH)_1]^{4-}$
1833.17	-4	$[\mathbf{L}^{\mathbf{S}}{}_2\mathbf{L}^{\mathbf{NO2}}{}_2(PO_4)_4[K(18\text{-}C\text{-}6)]_6K_2(H_2O)_1(CH_3CN)_1(DMSO)_1(CH_3OH)_1]^{4-}$
1845.68	-4	$[\mathbf{L}^{\mathbf{S}}{}_1\mathbf{L}^{\mathbf{NO2}}{}_3(PO_4)_4[K(18\text{-}C\text{-}6)]_6K_2(H_2O)_1(CH_3CN)_1(DMSO)_1(CH_3OH)_1]^{4-}$
1865.01	-4	$[\mathbf{L}^{\mathbf{S}}{}_4(PO_4)_4[K(18\text{-}C\text{-}6)]_7K_1(H_2O)_1(CH_3CN)_1(DMSO)_1]^{4-}$
1877.97	-4	$[\mathbf{L}^{\mathbf{S}}{}_3\mathbf{L}^{\mathbf{NO2}}{}_1(PO_4)_4[K(18\text{-}C\text{-}6)]_7K_1(H_2O)_1(CH_3CN)_1(DMSO)_1]^{4-}$
1890.68	-4	$[\mathbf{L}^{\mathbf{S}}{}_2\mathbf{L}^{\mathbf{NO2}}{}_2(PO_4)_4[K(18\text{-}C\text{-}6)]_7K_1(H_2O)_1(CH_3CN)_1(DMSO)_1]^{4-}$
1902.95	-4	$[\mathbf{L}^{\mathbf{S}}{}_1\mathbf{L}^{\mathbf{NO2}}{}_3(PO_4)_4[K(18\text{-}C\text{-}6)]_7K_1(H_2O)_1(CH_3CN)_1(DMSO)_1]^{4-}$
1915.65	-4	$[\mathbf{L}^{\mathbf{NO2}}{}_4(PO_4)_4[K(18\text{-}C\text{-}6)]_7K_1(H_2O)_1(CH_3CN)_1(DMSO)_1]^{4-}$

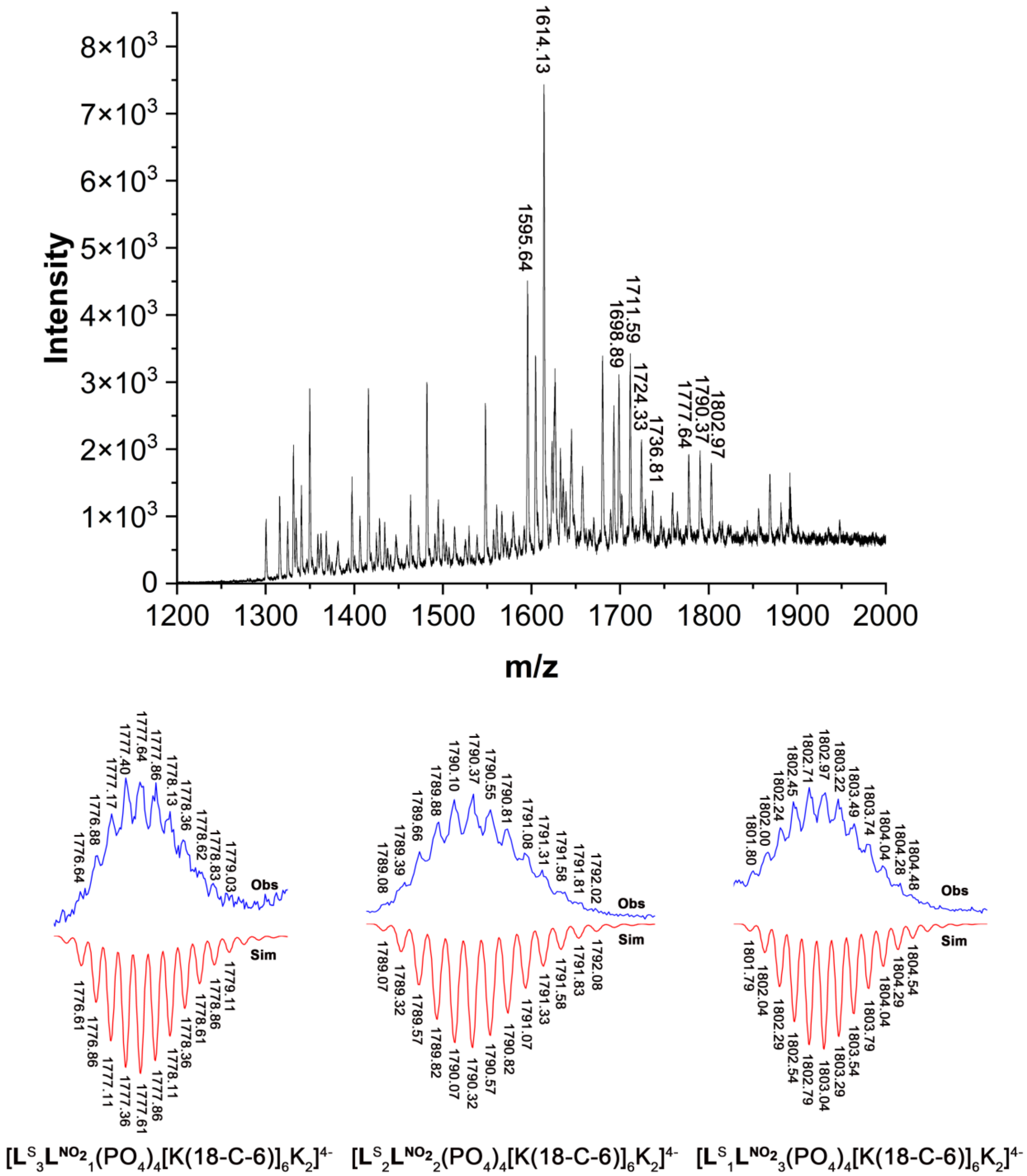

Figure S21. HR ESI-mass spectrum of phosphate-coordinated mixed-ligand cages ($\mathbf{L}^{S}$: $\mathbf{L}^{NO_2}$ = 3 : 1) in a mixed solvent of CH_3CN and DMSO (volume ratio of 9 : 1).

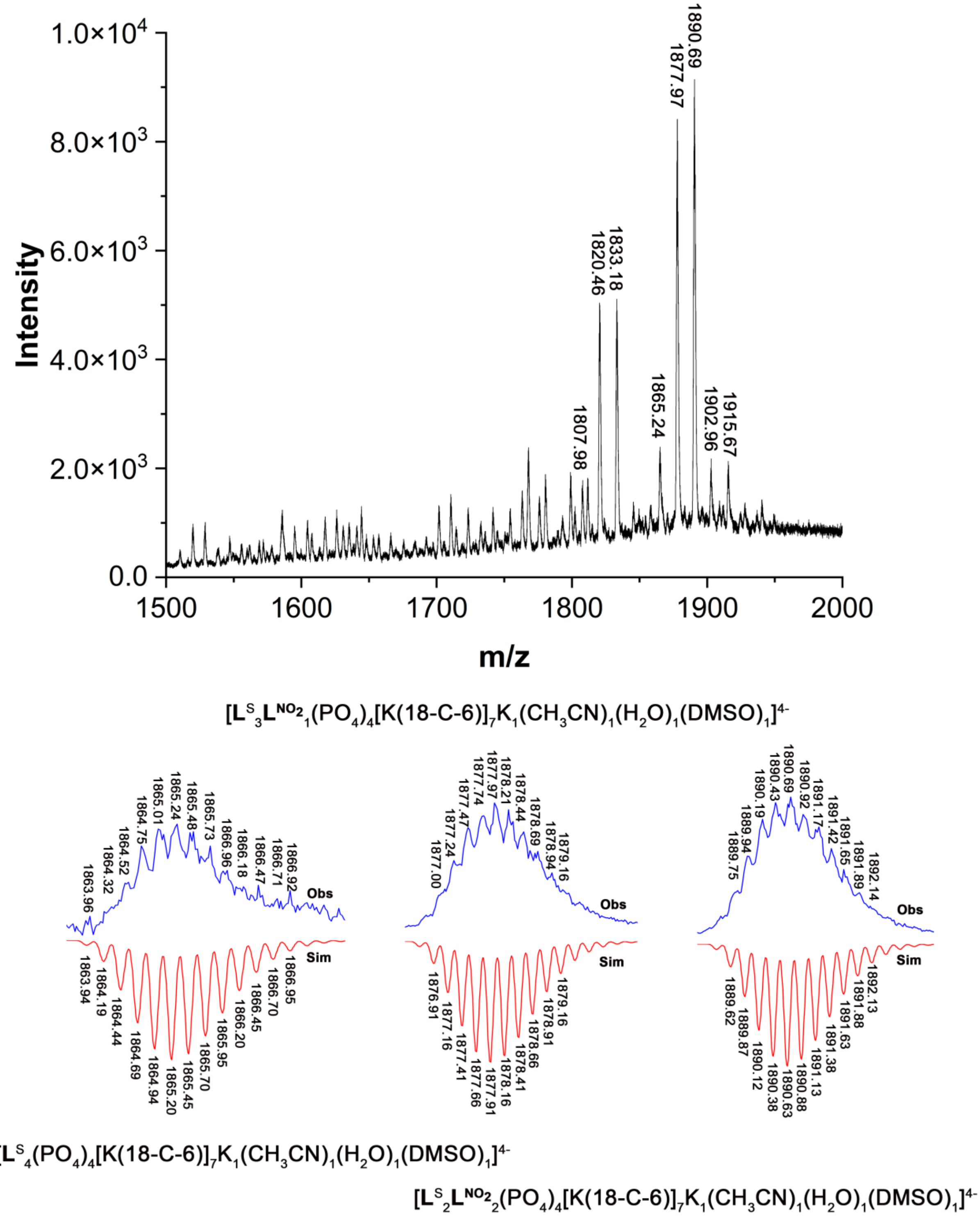

Figure S22. HR ESI-mass spectrum of phosphate-coordinated mixed-ligand cages ($\mathbf{L}^{\mathbf{S}}$: $\mathbf{L}^{\mathbf{NO_2}}$ = 3 : 1) with addition of TMA^+ in a mixed solvent of CH_3CN and DMSO (volume ratio of 9 : 1).

Table S6. The summary of HR ESI-MS data of the phosphate-coordinated mixed-ligand cages (**L**^{S} : **L**^{NO2} = 3 : 1) in a mixed solvent of CH_3CN and DMSO (volume ratio of 9 : 1).

m/z	*z*	**Formula**
1711.59	-4	$[L^{S}_{3}L^{NO2}_{1}(PO_4)_4[K(18\text{-}C\text{-}6)]_5K_3]^{4-}$
1724.33	-4	$[L^{S}_{2}L^{NO2}_{2}(PO_4)_4[K(18\text{-}C\text{-}6)]_5K_3]^{4-}$
1736.81	-4	$[L^{S}_{1}L^{NO2}_{3}(PO_4)_4[K(18\text{-}C\text{-}6)]_5K_3]^{4-}$
1777.64	-4	$[L^{S}_{3}L^{NO2}_{1}(PO_4)_4[K(18\text{-}C\text{-}6)]_6K_2]^{4-}$
1790.37	-4	$[L^{S}_{2}L^{NO2}_{2}(PO_4)_4[K(18\text{-}C\text{-}6)]_6K_2]^{4-}$
1802.97	-4	$[L^{S}_{1}L^{NO2}_{3}(PO_4)_4[K(18\text{-}C\text{-}6)]_6K_2]^{4-}$

Table S7. The summary of HR ESI-MS data of the phosphate-coordinated mixed-ligand cages (**L**^{S} : **L**^{NO2} = 3 : 1) with addition of TMA^+ in a mixed solvent of CH_3CN and DMSO (volume ratio of 9 : 1).

m/z	*z*	**Formula**
1807.98	-4	$[L^{S}_{4}(PO_4)_4[K(18\text{-}C\text{-}6)]_6K_2(H_2O)_1(CH_3CN)_1(DMSO)_1(CH_3OH)_1]^{4-}$
1820.46	-4	$[L^{S}_{3}L^{NO2}_{1}(PO_4)_4[K(18\text{-}C\text{-}6)]_6K_2(H_2O)_1(CH_3CN)_1(DMSO)_1(CH_3OH)_1]^{4-}$
1833.18	-4	$[L^{S}_{2}L^{NO2}_{2}(PO_4)_4[K(18\text{-}C\text{-}6)]_6K_2(H_2O)_1(CH_3CN)_1(DMSO)_1(CH_3OH)_1]^{4-}$
1865.24	-4	$[L^{S}_{4}(PO_4)_4[K(18\text{-}C\text{-}6)]_7K_1(H_2O)_1(CH_3CN)_1(DMSO)_1]^{4-}$
1877.97	-4	$[L^{S}_{3}L^{NO2}_{1}(PO_4)_4[K(18\text{-}C\text{-}6)]_7K_1(H_2O)_1(CH_3CN)_1(DMSO)_1]^{4-}$
1890.69	-4	$[L^{S}_{2}L^{NO2}_{2}(PO_4)_4[K(18\text{-}C\text{-}6)]_7K_1(H_2O)_1(CH_3CN)_1(DMSO)_1]^{4-}$
1902.96	-4	$[L^{S}_{1}L^{NO2}_{3}(PO_4)_4[K(18\text{-}C\text{-}6)]_7K_1(H_2O)_1(CH_3CN)_1(DMSO)_1]^{4-}$
1915.67	-4	$[L^{NO2}_{4}(PO_4)_4[K(18\text{-}C\text{-}6)]_7K_1(H_2O)_1(CH_3CN)_1(DMSO)_1]^{4-}$

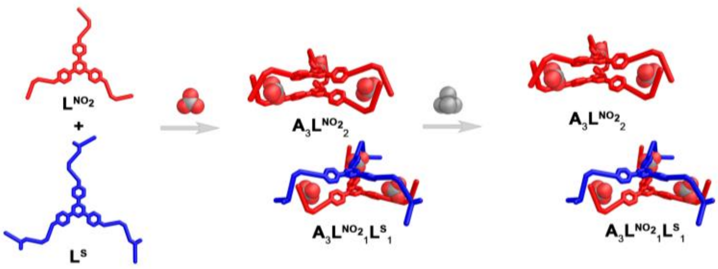

Scheme S2. Schematic representation of the self-assembly of carbonate-coordinated mixed-ligand (**L**^{S} : **L**^{NO2} = 1 : 3) structures and the subsequent addition of TMA^+ ion.

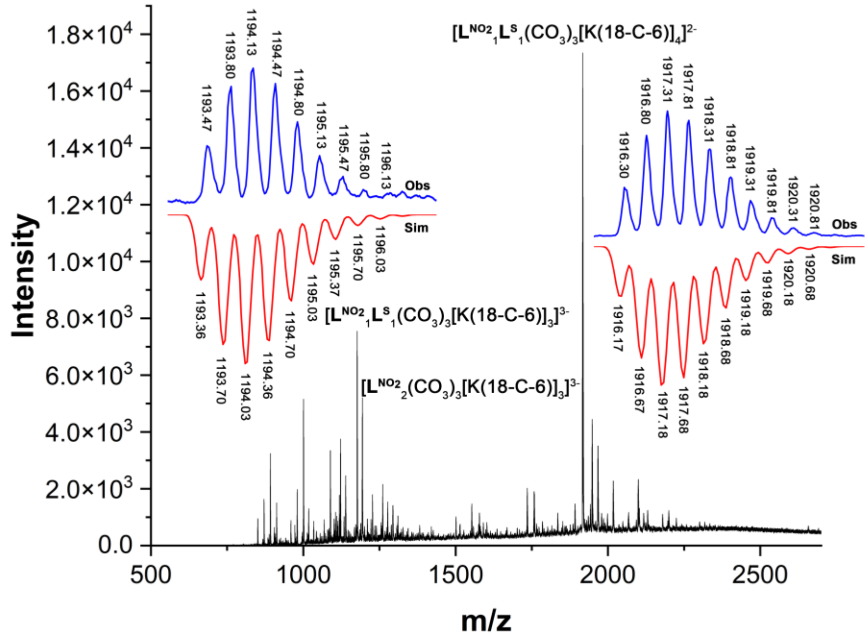

Figure S23. HR ESI-mass spectrum of the carbonate-coordinated mixed-ligand structures ($\mathbf{L^S}$: $\mathbf{L^{NO2}}$ = 1 : 3) in a mixed solvent of CH_3CN and DMSO (volume ratio of 9 : 1).

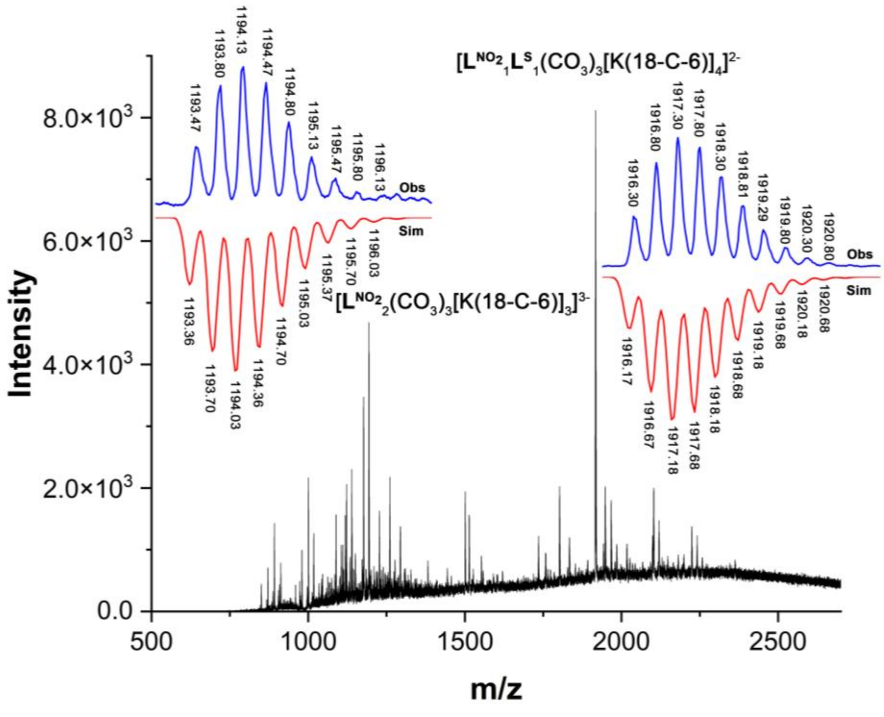

Figure S24. HR ESI-mass spectrum of the carbonate-coordinated mixed-ligand structures ($\mathbf{L^S}$: $\mathbf{L^{NO2}}$ = 1 : 3) with addition of TMA^+ in a mixed solvent of CH_3CN and DMSO (volume ratio of 9 : 1).

Table S8. The summary of HR ESI-MS data of the carbonate-coordinated mixed-ligand structures ($\mathbf{L^S}$: $\mathbf{L^{NO2}}$ = 1 : 3) in a mixed solvent of CH_3CN and DMSO (volume ratio of 9 : 1).

m/z	*z*	**Formula**
1177.10	-3	$[\mathbf{L^S}_1\mathbf{L^{NO2}}_1(CO_3)_3[K(18\text{-}C\text{-}6)]_3]^{3-}$
1194.13	-3	$[\mathbf{L^{NO2}}_2(CO_3)_3[K(18\text{-}C\text{-}6)]_3]^{3-}$
1917.31	-2	$[\mathbf{L^S}_1\mathbf{L^{NO2}}_1(CO_3)_3[K(18\text{-}C\text{-}6)]_4]^{2-}$

Table S9. The summary of HR ESI-MS data of the carbonate-coordinated mixed-ligand structures ($\mathbf{L^S}$: $\mathbf{L^{NO2}}$ = 1 : 3) with addition of TMA^+ in a mixed solvent of CH_3CN and DMSO (volume ratio of 9 : 1).

m/z	*z*	**Formula**
1177.10	-3	$[\mathbf{L^S}_1\mathbf{L^{NO2}}_1(CO_3)_3[K(18\text{-}C\text{-}6)]_3]^{3-}$
1194.13	-3	$[\mathbf{L^{NO2}}_2(CO_3)_3[K(18\text{-}C\text{-}6)]_3]^{3-}$
1917.30	-2	$[\mathbf{L^S}_1\mathbf{L^{NO2}}_1(CO_3)_3[K(18\text{-}C\text{-}6)]_4]^{2-}$

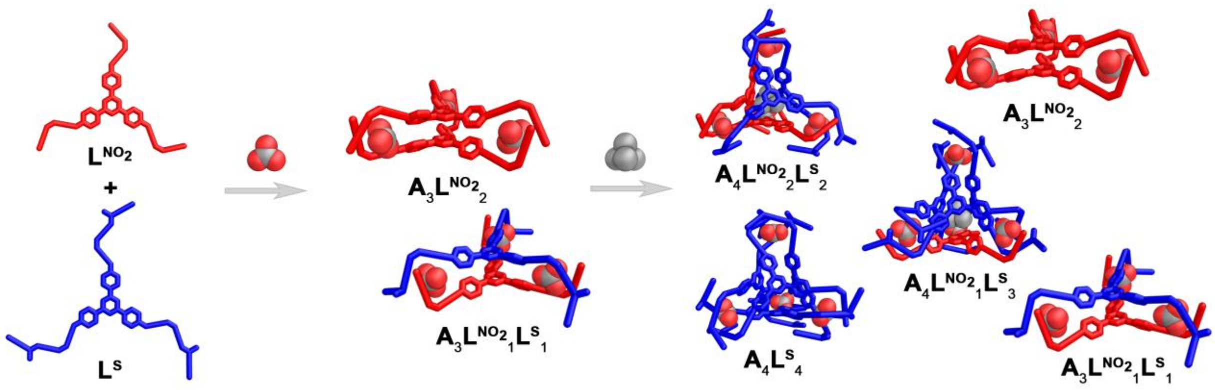

Scheme S3. Schematic representation of the self-assembly of carbonate-coordinated mixed-ligand ($\mathbf{L^S}$: $\mathbf{L^{NO2}}$ = 1 : 1 and 3 : 1) structures and the subsequent addition of TMA^+ ion.

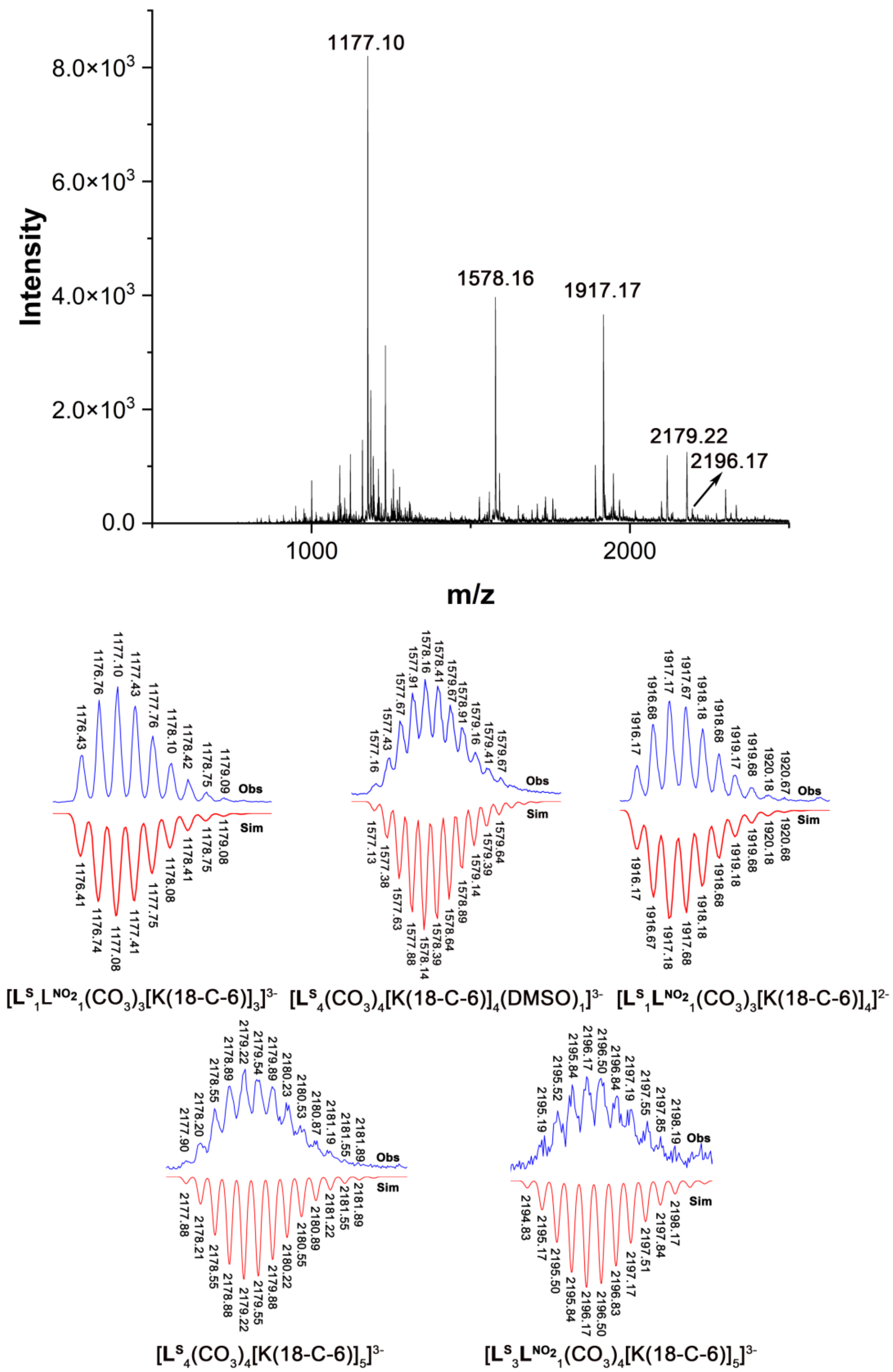

Figure S25. HR ESI-mass spectrum of the carbonate-coordinated mixed-ligand structures (**L**^{S} : **L**^{NO_2} = 1 : 1) in a mixed solvent of CH_3CN and DMSO (volume ratio of 9 : 1).

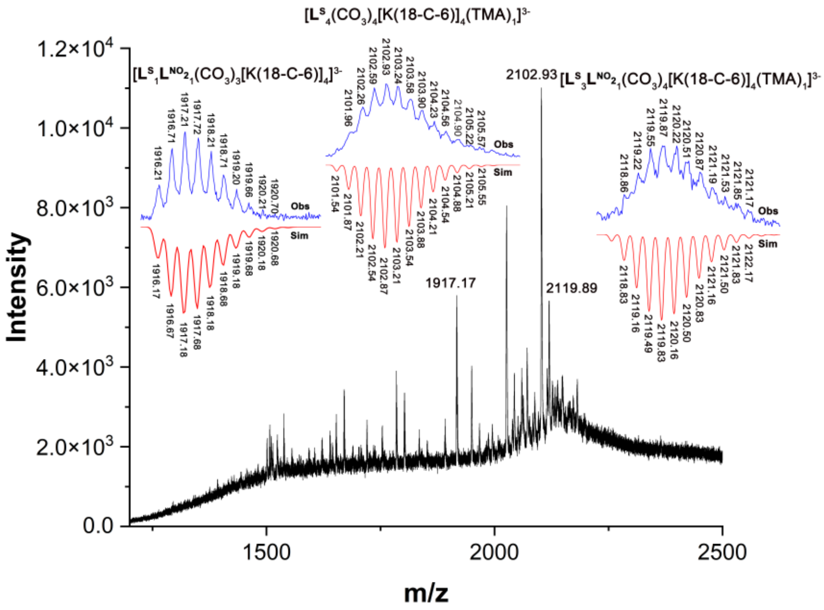

Figure S26. HR ESI-mass spectrum of the carbonate-coordinated mixed-ligand structures ($\mathbf{L^S}$: $\mathbf{L^{NO2}}$ = 1 : 1) with addition of TMA$^+$ in a mixed solvent of CH_3CN and DMSO (volume ratio of 9 : 1).

Table S10. The summary of HR ESI-MS data of the carbonate-coordinated mixed-ligand structures ($\mathbf{L^S}$: $\mathbf{L^{NO2}}$ = 1 : 1) in a mixed solvent of CH_3CN and DMSO (volume ratio of 9 : 1).

m/z	*z*	**Formula**
1177.10	-3	$[\mathbf{L^S}_1\mathbf{L^{NO2}}_1(CO_3)_3[K(18\text{-}C\text{-}6)]_3]^{3-}$
1578.16	-4	$[\mathbf{L^S}_4(CO_3)_4[K(18\text{-}C\text{-}6)]_4(DMSO)_1]^{4-}$
1917.17	-2	$[\mathbf{L^S}_1\mathbf{L^{NO2}}_1(CO_3)_3[K(18\text{-}C\text{-}6)]_4]^{2-}$
2179.22	-3	$[\mathbf{L^S}_4(CO_3)_4[K(18\text{-}C\text{-}6)]_5]^{3-}$
2196.17	-3	$[\mathbf{L^S}_3\mathbf{L^{NO2}}_1(CO_3)_4[K(18\text{-}C\text{-}6)]_5]^{3-}$

Table S11. The summary of HR ESI-MS data of the carbonate-coordinated mixed-ligand structures ($\mathbf{L^S}$: $\mathbf{L^{NO2}}$ = 1 : 1) with addition of TMA$^+$ in a mixed solvent of CH_3CN and DMSO (volume ratio of 9 : 1).

m/z	*z*	**Formula**
2102.93	-3	$[\mathbf{L^S}_4(CO_3)_4[K(18\text{-}C\text{-}6)]_4(TMA)]^{3-}$
1917.21	-2	$[\mathbf{L^S}_1\mathbf{L^{NO2}}_1(CO_3)_3[K(18\text{-}C\text{-}6)]_4]^{2-}$
2119.87	-3	$[\mathbf{L^S}_3\mathbf{L^{NO2}}_1(CO_3)_4[K(18\text{-}C\text{-}6)]_4(TMA)]^{3-}$

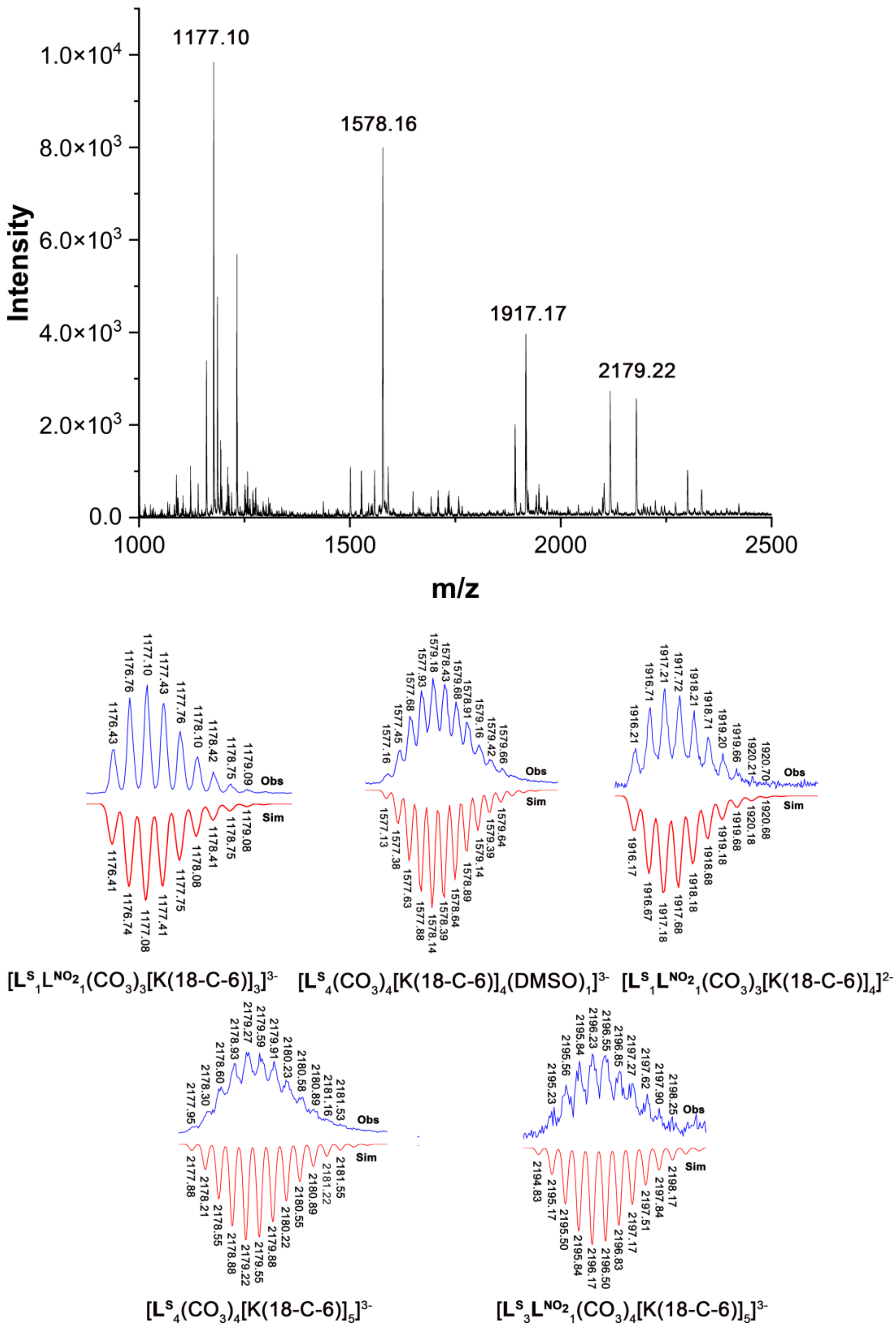

Figure S27. HR ESI-mass spectrum of the carbonate-coordinated mixed-ligand structures (**L**$^{\mathbf{S}}$: **L**$^{\mathbf{NO2}}$ = 3 : 1) in a mixed solvent of CH_3CN and DMSO (volume ratio of 9 : 1).

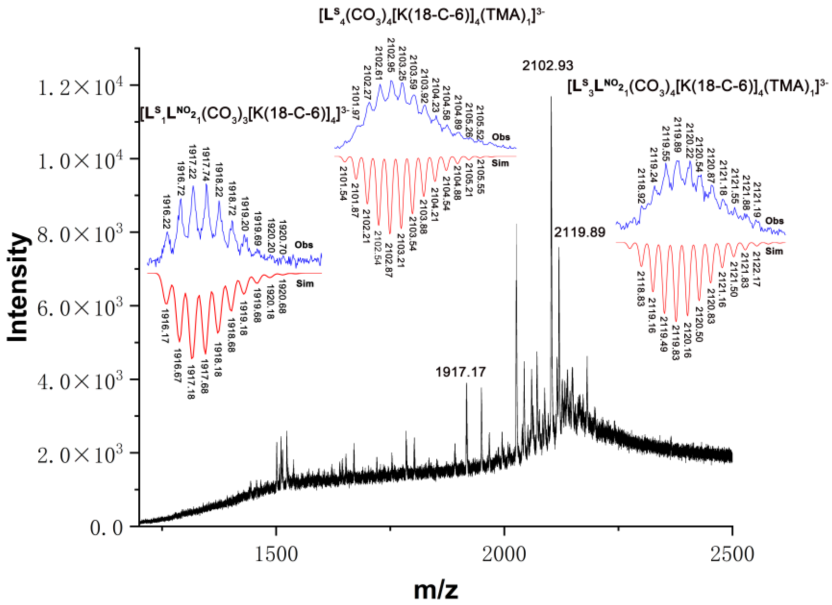

Figure S28. HR ESI-mass spectrum of the carbonate-coordinated mixed-ligand structures ($\mathbf{L^{S}}$: $\mathbf{L^{NO2}}$ = 3 : 1) with addition of TMA^{+} in a mixed solvent of CH_3CN and DMSO (volume ratio of 9 : 1).

Table S12. The summary of HR ESI-MS data of the carbonate-coordinated mixed-ligand structures ($\mathbf{L^{S}}$: $\mathbf{L^{NO2}}$ = 3 : 1) in a mixed solvent of CH_3CN and DMSO (volume ratio of 9 : 1).

m/z	*z*	**Formula**
1177.10	-3	$[\mathbf{L^{S}}_1\mathbf{L^{NO2}}_1(CO_3)_3[K(18\text{-}C\text{-}6)]_3]^{3-}$
1578.18	-4	$[\mathbf{L^{S}}_4(CO_3)_4[K(18\text{-}C\text{-}6)]_4(DMSO)_1]^{4-}$
1917.21	-2	$[\mathbf{L^{S}}_1\mathbf{L^{NO2}}_1(CO_3)_3[K(18\text{-}C\text{-}6)]_4]^{2-}$
2179.27	-3	$[\mathbf{L^{S}}_4(CO_3)_4[K(18\text{-}C\text{-}6)]_5]^{3-}$
2196.23	-3	$[\mathbf{L^{S}}_3\mathbf{L^{NO2}}_1(CO_3)_4[K(18\text{-}C\text{-}6)]_5]^{3-}$

Table S13. The summary of HR ESI-MS data of the carbonate-coordinated mixed-ligand structures ($\mathbf{L^{S}}$: $\mathbf{L^{NO2}}$ = 3 : 1) with addition of TMA^{+} in a mixed solvent of CH_3CN and DMSO (volume ratio of 9 : 1).

m/z	*z*	**Formula**
2102.95	-3	$[\mathbf{L^{S}}_4(CO_3)_4[K(18\text{-}C\text{-}6)]_4(TMA)]^{3-}$
1917.22	-2	$[\mathbf{L^{S}}_1\mathbf{L^{NO2}}_1(CO_3)_3[K(18\text{-}C\text{-}6)]_4]^{2-}$
2119.89	-3	$[\mathbf{L^{S}}_3\mathbf{L^{NO2}}_1(CO_3)_4[K(18\text{-}C\text{-}6)]_4(TMA)]^{3-}$

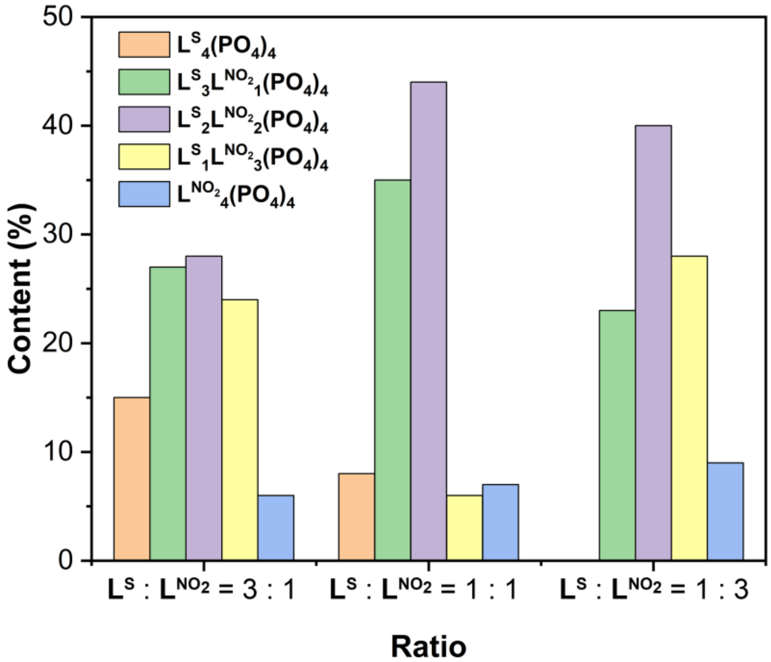

Figure S29. The percentage content of the formed phosphate-coordinated mixed-ligand cages in different mixing ratios of $\mathbf{L}^{\mathbf{NO2}}$ and $\mathbf{L}^{\mathbf{S}}$.

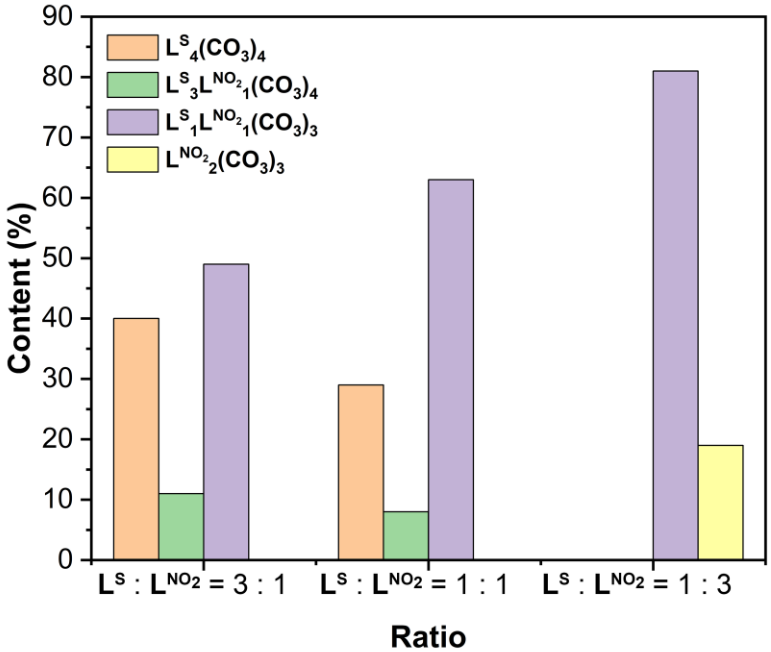

Figure S30. The percentage content of the formed carbonate-coordinated mixed-ligand cages in different mixing ratios of $\mathbf{L}^{\mathbf{NO2}}$ and $\mathbf{L}^{\mathbf{S}}$.

S4. NMR studies

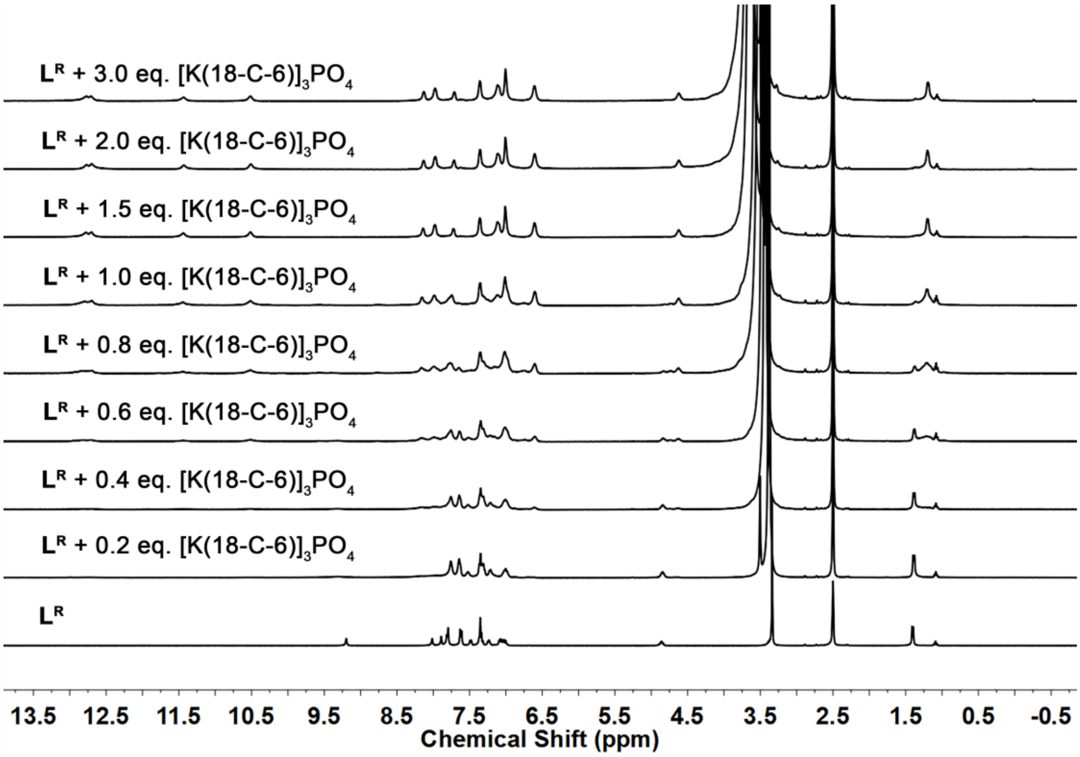

Figure S31. ^1H NMR spectra (400 MHz, DMSO-d_6, 298 K) of $\mathbf{L^R}$ upon addition of $[K(18\text{-}C\text{-}6)]_3PO_4$.

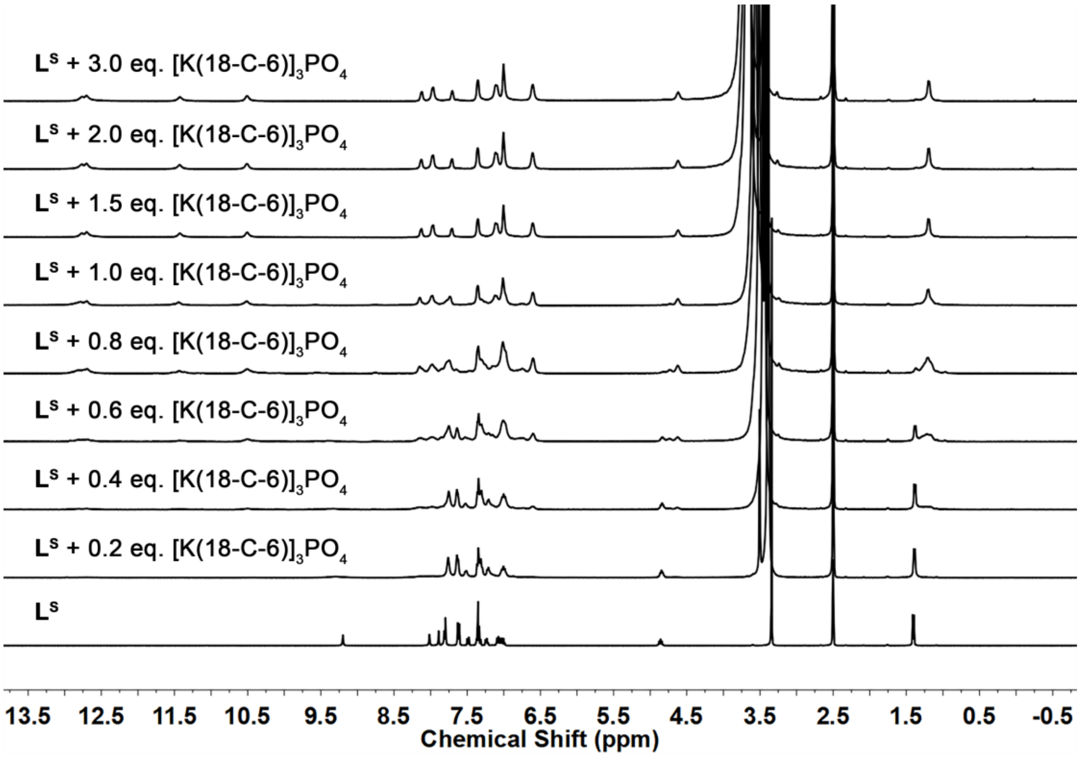

Figure S32. ^1H NMR spectra (400 MHz, DMSO-d_6, 298 K) of $\mathbf{L^S}$ upon addition of $[K(18\text{-}C\text{-}6)]_3PO_4$.

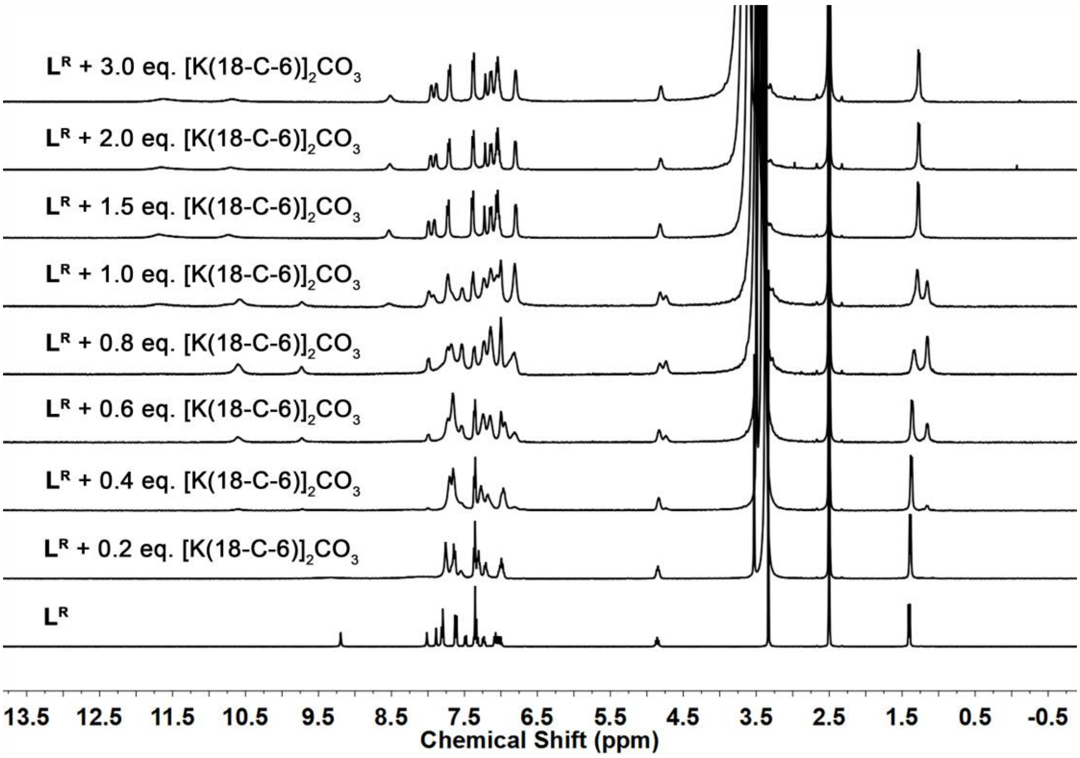

Figure S33. ^{1}H NMR spectra (400 MHz, DMSO-d_6, 298 K) of $\mathbf{L^R}$ upon addition of $[K(18\text{-}C\text{-}6)]_2CO_3$.

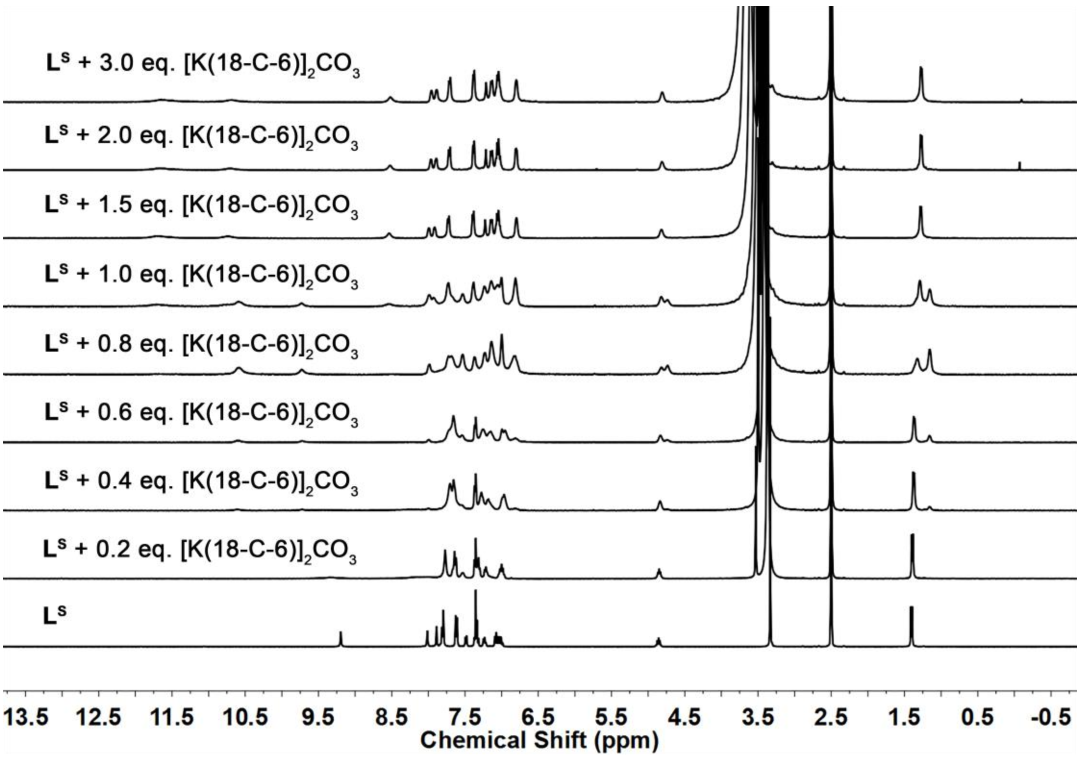

Figure S34. ^{1}H NMR spectra (400 MHz, DMSO-d_6, 298 K) of $\mathbf{L^S}$ upon addition of $[K(18\text{-}C\text{-}6)]_2CO_3$.

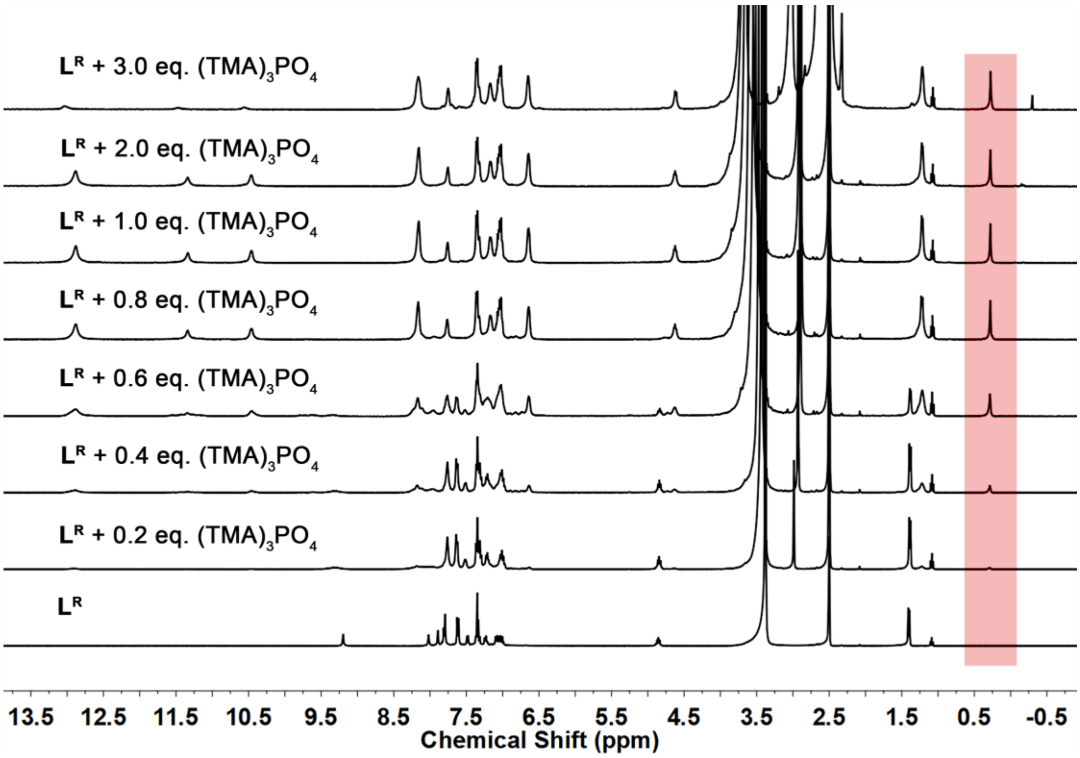

Figure S35. ^{1}H NMR spectra (400 MHz, DMSO-d_6, 298 K) of $\mathbf{L^R}$ upon addition of $(TMA)_3PO_4$.

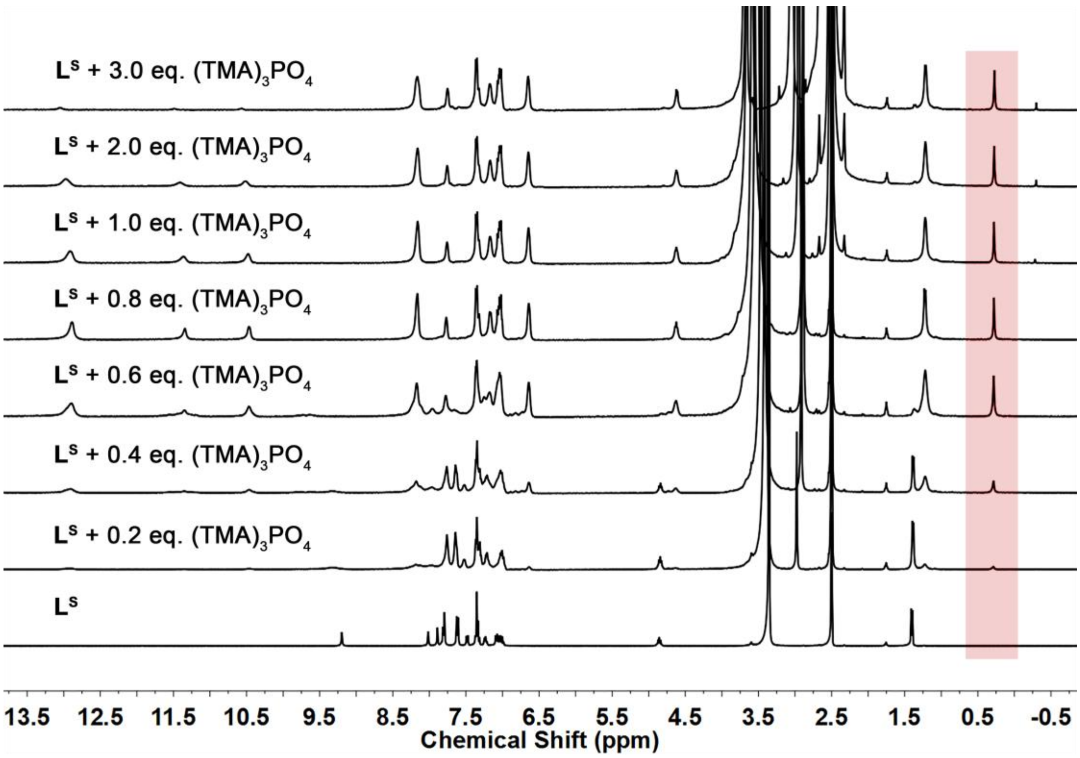

Figure S36. ^{1}H NMR spectra (400 MHz, DMSO-d_6, 298 K) of $\mathbf{L^S}$ upon addition of $(TMA)_3PO_4$.

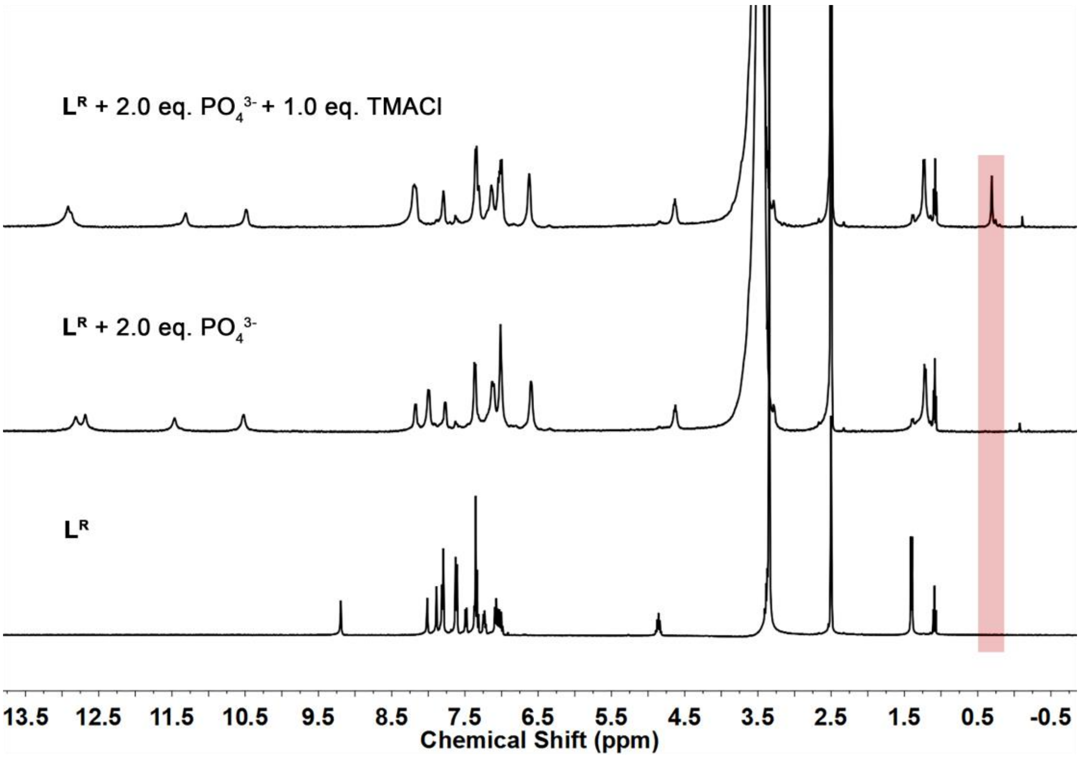

Figure S37. [1]H NMR spectra (400 MHz, DMSO-d_6, 298 K) of $\mathbf{L^R}$, $\mathbf{L^R}$ with addition of 2.0 eq. $[K(18\text{-}C\text{-}6)]_3PO_4$, and subsequent addition of 1.0 eq. TMACl.

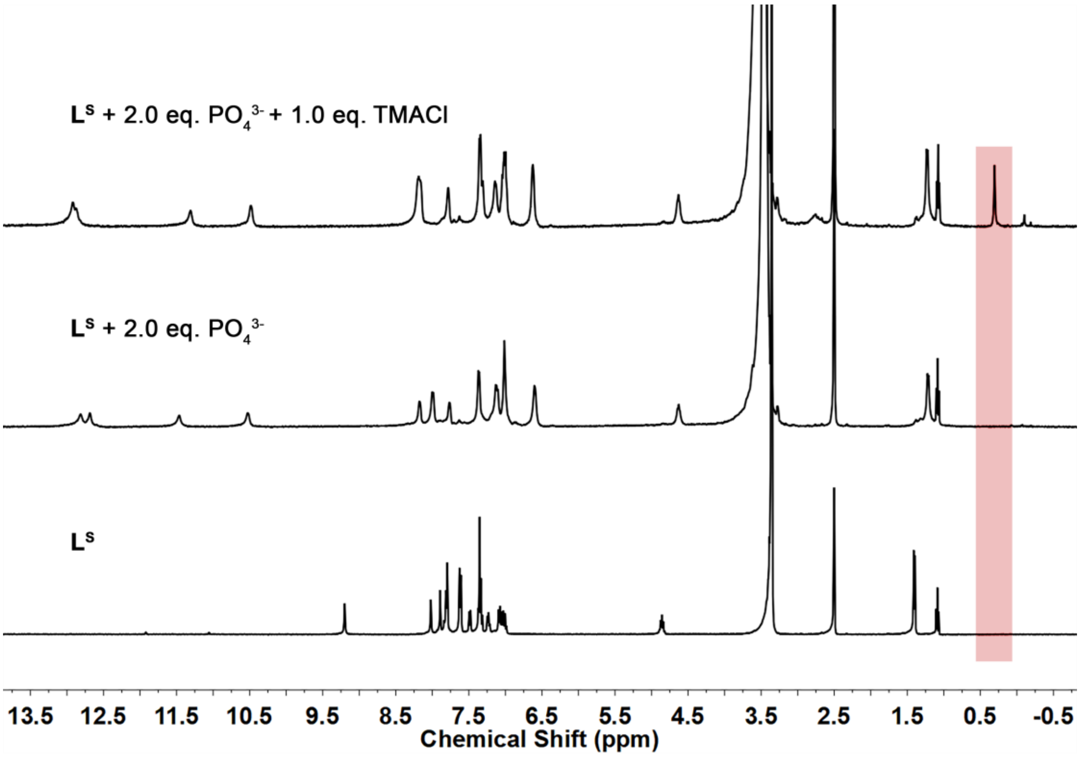

Figure S38. [1]H NMR spectra (400 MHz, DMSO-d_6, 298 K) of $\mathbf{L^S}$, $\mathbf{L^S}$ with addition of 2.0 eq. $[K(18\text{-}C\text{-}6)]_3PO_4$, and subsequent addition of 1.0 eq. TMACl.

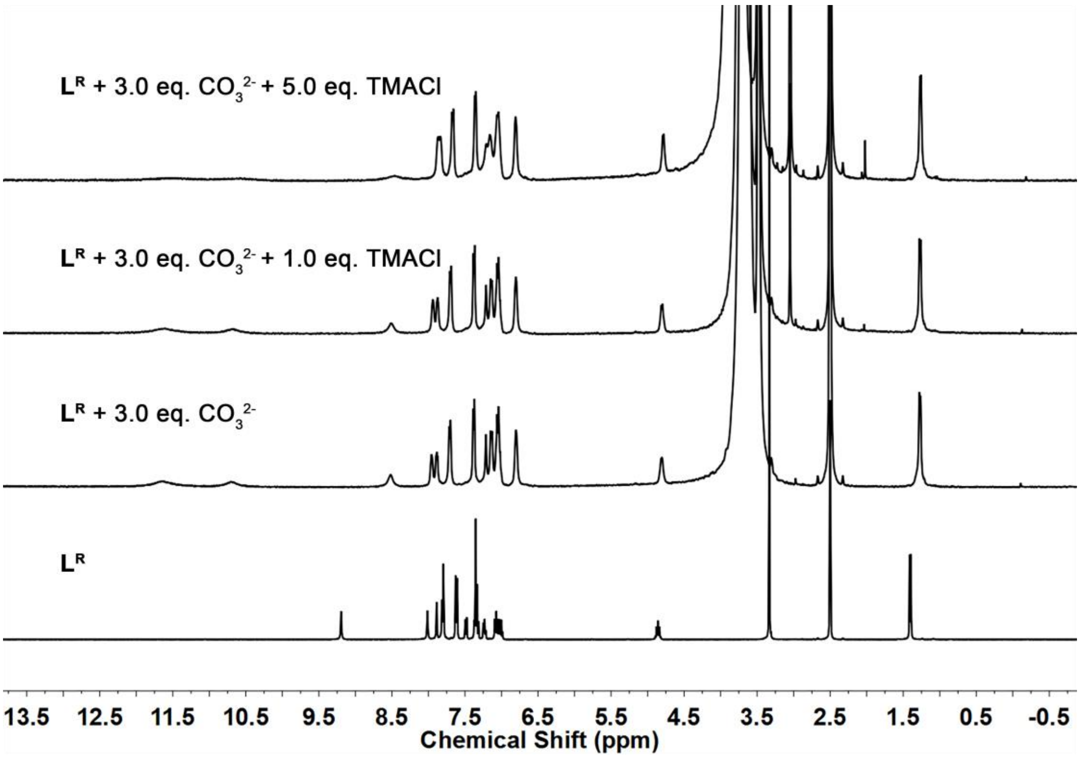

Figure S39. ^{1}H NMR spectra (400 MHz, DMSO-d_6, 298 K) of $\mathbf{L^R}$, $\mathbf{L^R}$ with addition of 3.0 eq. $[K(18\text{-}C\text{-}6)]_2CO_3$, and subsequent addition of 5.0 eq. TMACl.

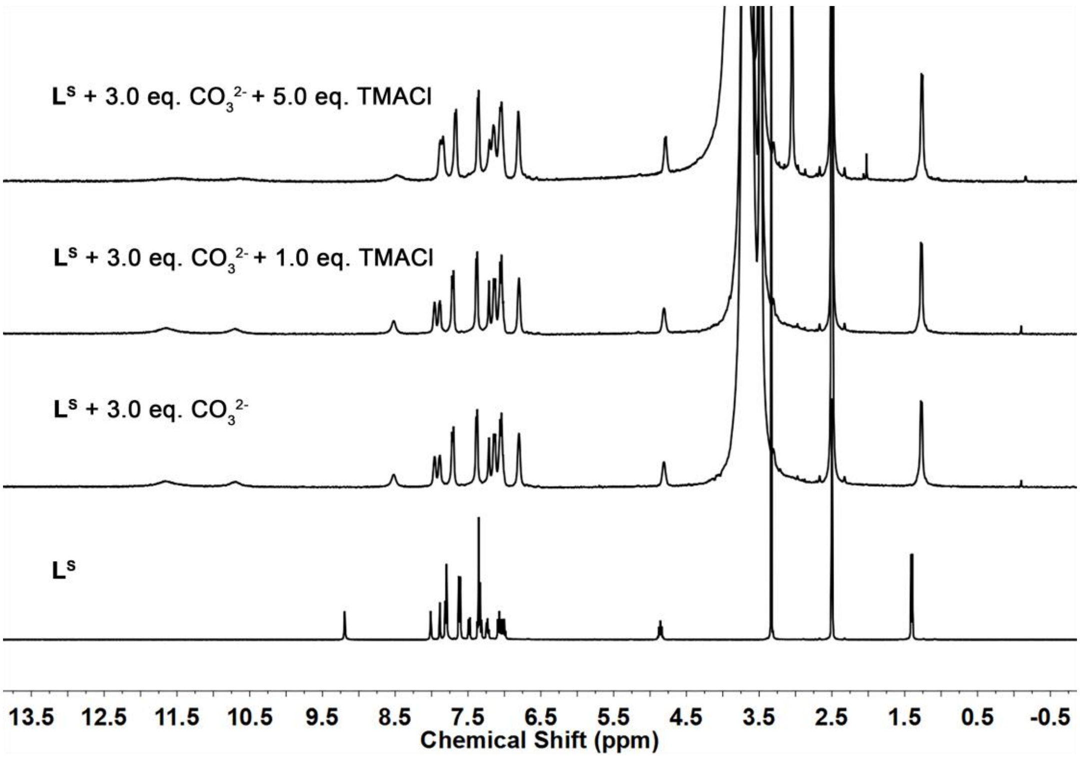

Figure S40. ^{1}H NMR spectra (400 MHz, DMSO-d_6, 298 K) of $\mathbf{L^S}$, $\mathbf{L^S}$ upon addition of 3.0 eq. $[K(18\text{-}C\text{-}6)]_2CO_3$, and subsequent addition of 5.0 eq. TMACl.

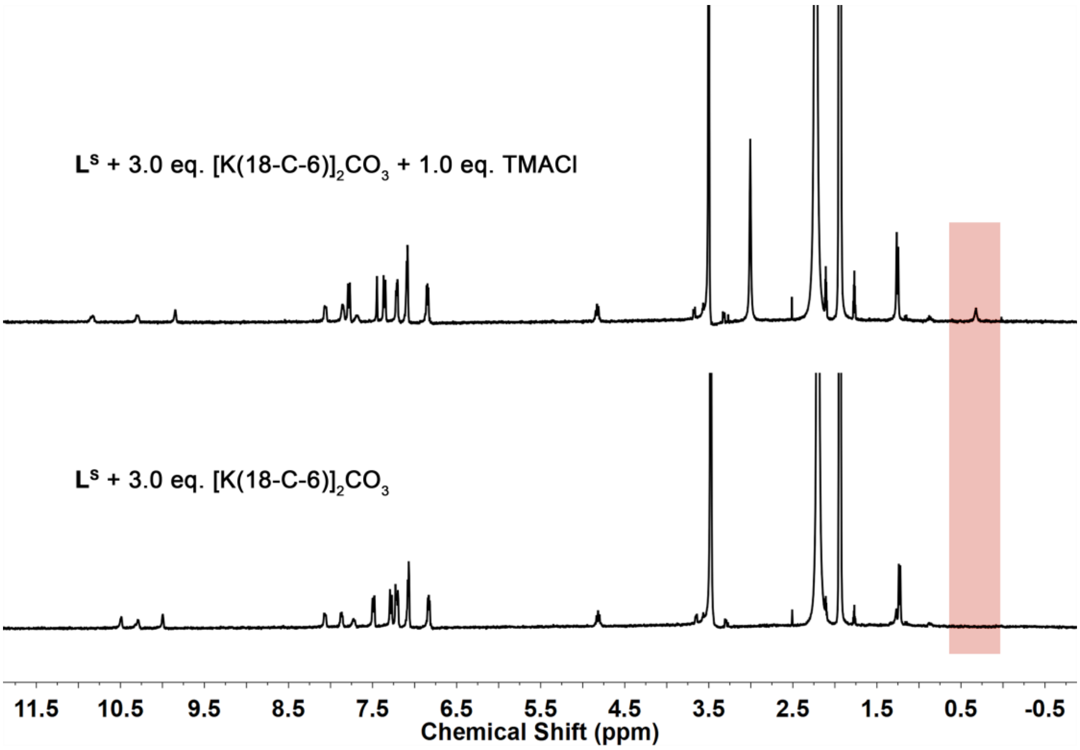

Figure S41. ^{1}H NMR spectra (400 MHz, acetonitrile-d_3, 298 K) of $\mathbf{L^S}$ with addition of 3.0 eq. [K(18-C-6)]$_2$CO$_3$ and subsequent addition of 1.0 eq. TMACl.

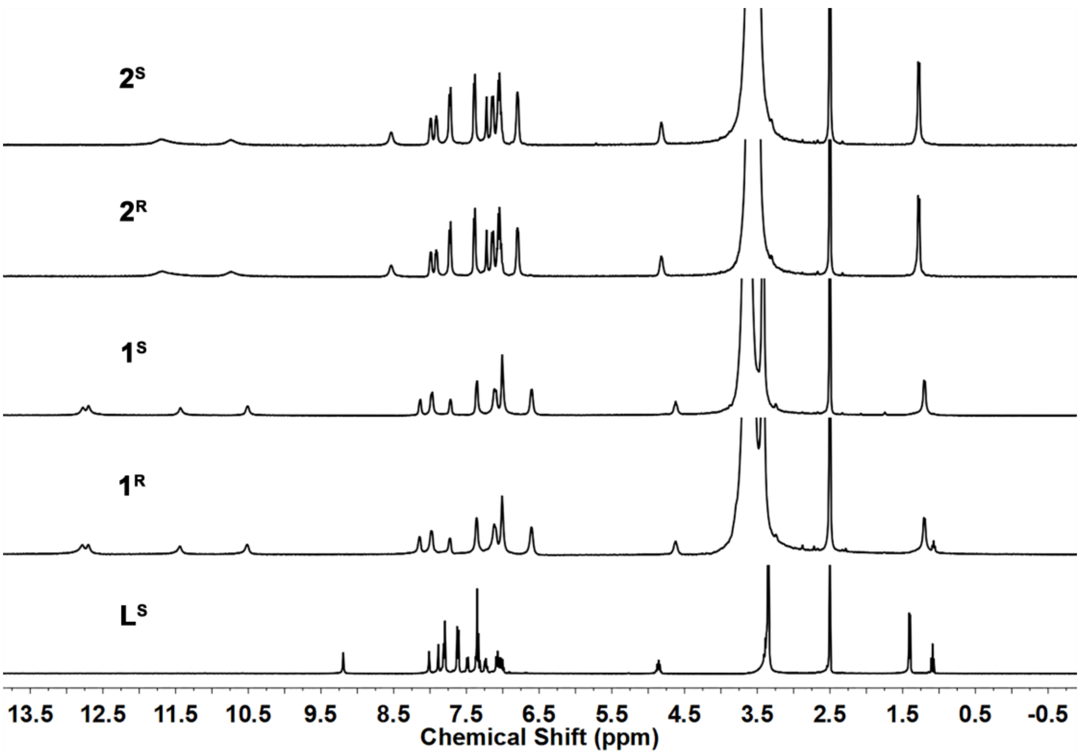

Figure S42. ^{1}H NMR spectra (400 MHz, DMSO-d_6, 298 K) of $\mathbf{L^S}$, $\mathbf{1^{R/S}}$, and $\mathbf{2^{R/S}}$.

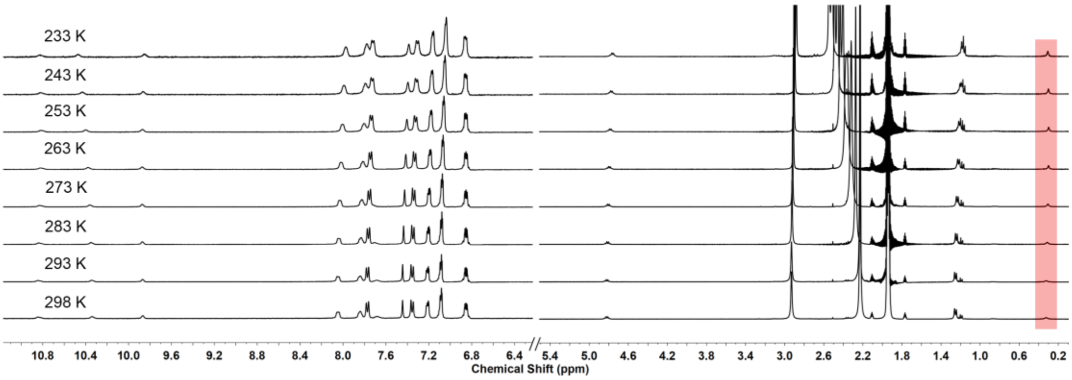

Figure S43. Variable temperature [1]H NMR spectra (400 MHz, acetonitrile-d_3, 298 K to 233 K, the signal of trapped TMA^+ was highlighted by red rectangle) of $(CO_3)_4$**L**$^{\mathbf{S}}_4$ (generated from **L**$^{\mathbf{S}}$ and $(TMA)_2CO_3$).

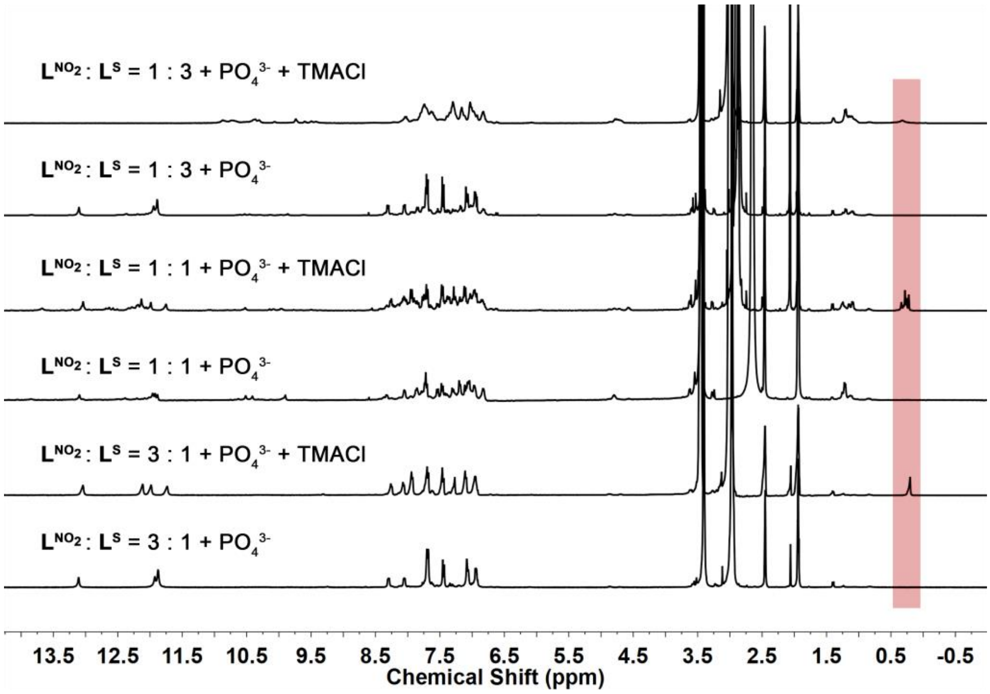

Figure S44. [1]H NMR spectra (400 MHz, DMSO-d_6, 298 K) of phosphate-coordinated mixed-ligand (**L**$^{\mathbf{S}}$: **L**$^{\mathbf{NO2}}$ = 1 : 3, **L**^{S} : **L**$^{\mathbf{NO2}}$ = 1 : 1, **L**^{S} : **L**$^{\mathbf{NO2}}$ = 3 : 1) cages (self-assembly with 10 eq. $[K(18\text{-}C\text{-}6)]_3PO_4$), and subsequent addition of 1 eq. TMACl.

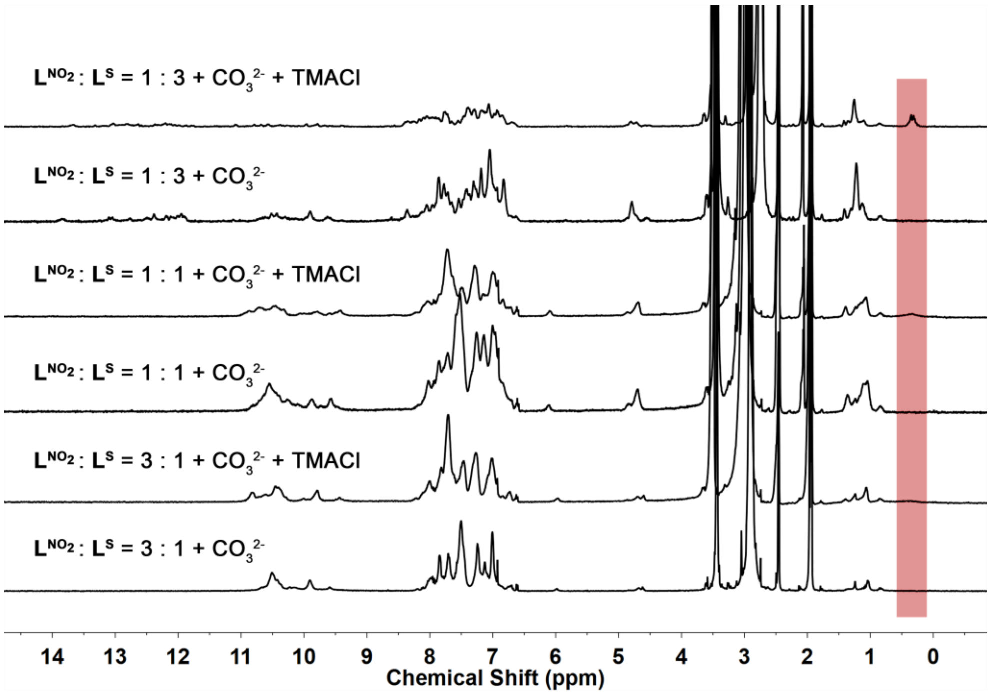

Figure S45. [1]H NMR spectra (400 MHz, DMSO-d_6, 298 K) of carbonate-coordinated mixed-ligand (**L**^{S} : **L**^{NO2} = 1 : 3, **L**^{S} : **L**^{NO2} = 1 : 1, **L**^{S} : **L**^{NO2} = 3 : 1) cages (self-assembly with 10 eq. $[K(18\text{-}C\text{-}6)]_2CO_3$), and subsequent addition of 1 eq. TMACl.

S5. UV-vis characterization

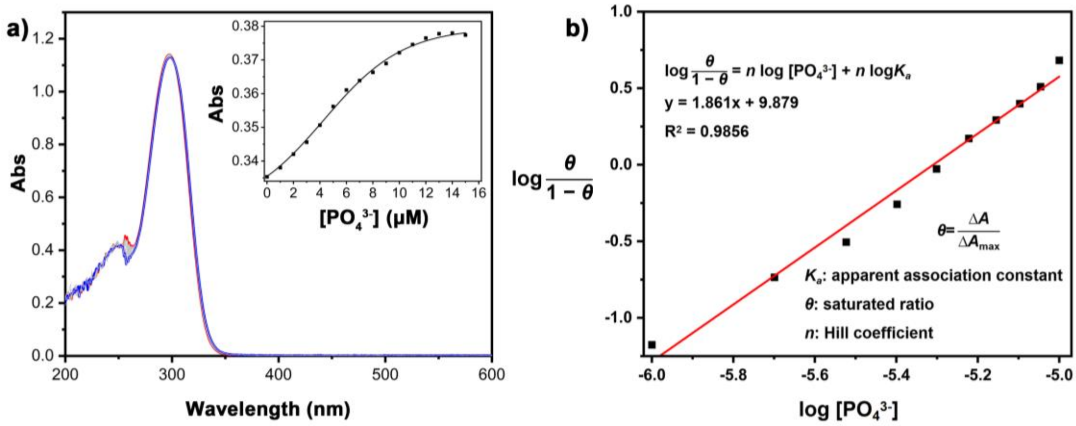

Figure S46. a) UV-vis spectra of **L**^{S} (0.05 mM) in DMSO upon addition of $[K(18\text{-}C\text{-}6)]_3PO_4$. b) Titration curve of **L**^{S} vs PO_4^{3-} with Hill function.

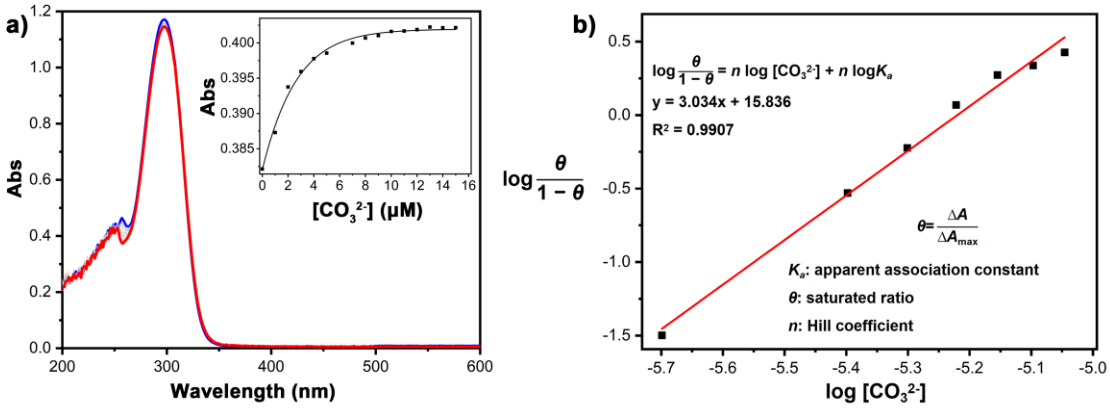

Figure S47. a) UV-vis spectra of $\mathbf{L^S}$ (0.05 mM) in DMSO upon addition of [K(18-C-6)]$_3$CO$_3$. b) Titration curve of $\mathbf{L^S}$ vs CO_3^{2-} with Hill function.

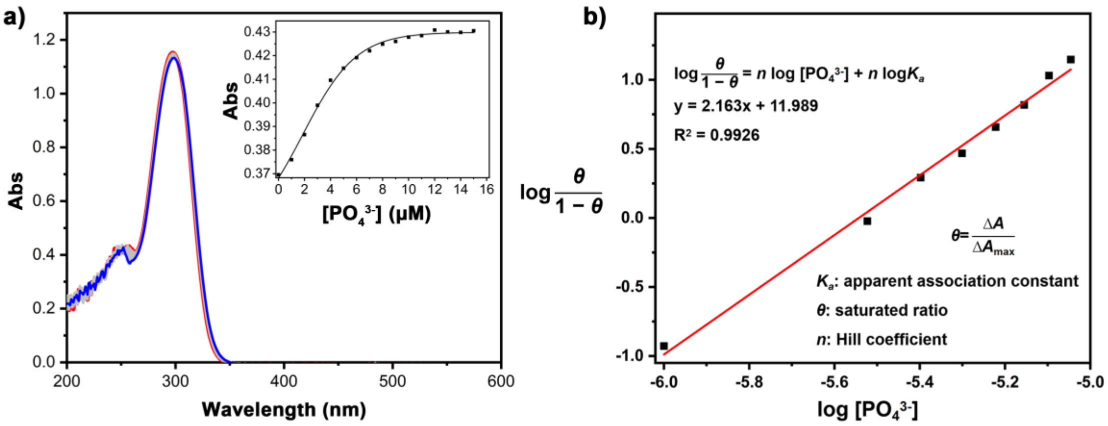

Figure S48. a) UV-vis spectra of $\mathbf{L^S}$ (0.05 mM) in DMSO upon addition of (TMA)$_3$PO$_4$. b) Titration curve of $\mathbf{L^S}$ vs (TMA)$_3$PO$_4$ with Hill function.

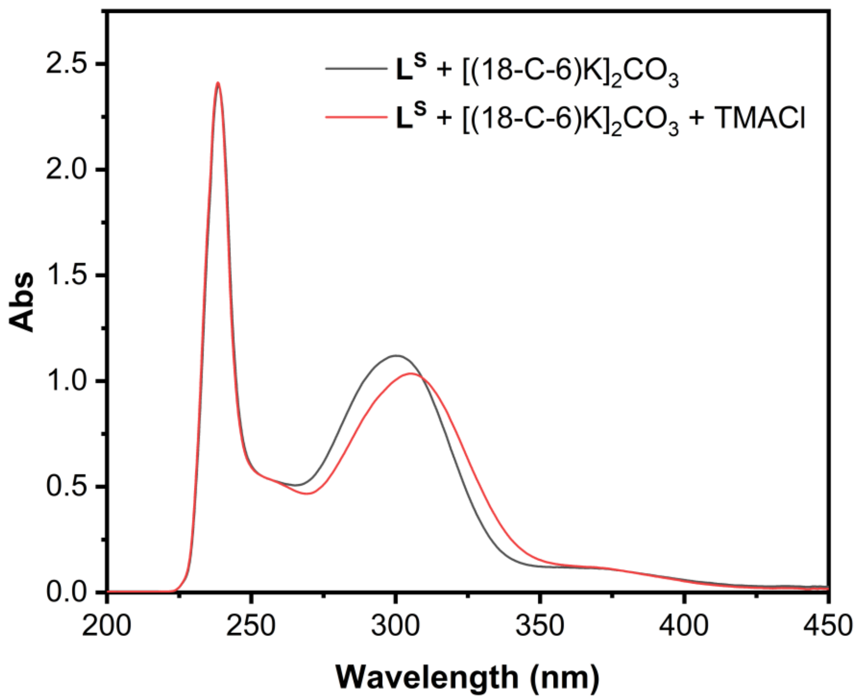

Figure S49. UV-vis spectra of $\mathbf{L}^S$ with $[(18\text{-}C\text{-}6)K]_2CO_3$, $\mathbf{L}^S$ with $[(18\text{-}C\text{-}6)K]_2CO_3$ and subsequent addition of 1 eq. TMACl.

S6. Theoretical Calculations

Geometry optimizations for $\mathbf{1}^{R/S}$, $\mathbf{3}^{R/S}$ and corresponding host-guest complexes by the Geometry, Frequency, Non-Covalent Extended Tight-Binding (GFN2-xTB) method[2] were peformed using version 6.4.4 of the xTB code (https://github.com/grimme-lab/xtb). Based on the xTB optimized geometries, the CD optical properties were computed by the simplified Tamm-Dancoff approach[3] employing version 1.6.3.3 of the sTDA code (https://github.com/grimme-lab/stda). An empirical factor were scaled to the simulated CD peak to align with the experimental CD spectra. Meanwhile, the volume of the internal cavity of $\mathbf{1}^{R/S}$ and $\mathbf{3}^{R/S}$ were estimated by the MoloVol program (1.4 Å probe).[4]

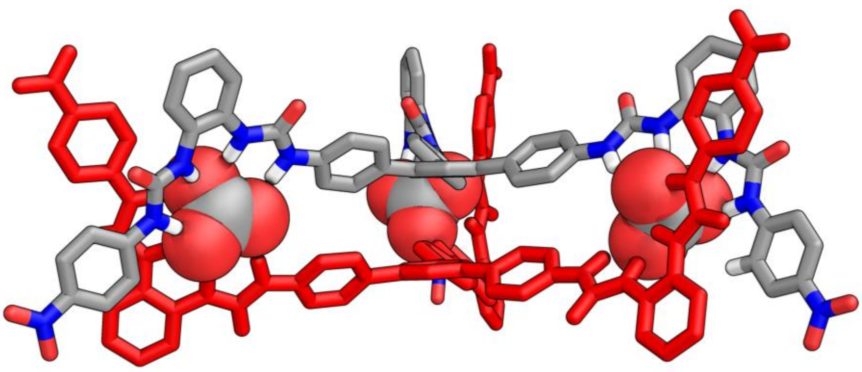

Figure S50. Molecular models of $\mathbf{L}^{NO2}$ with CO_3^{2-}.

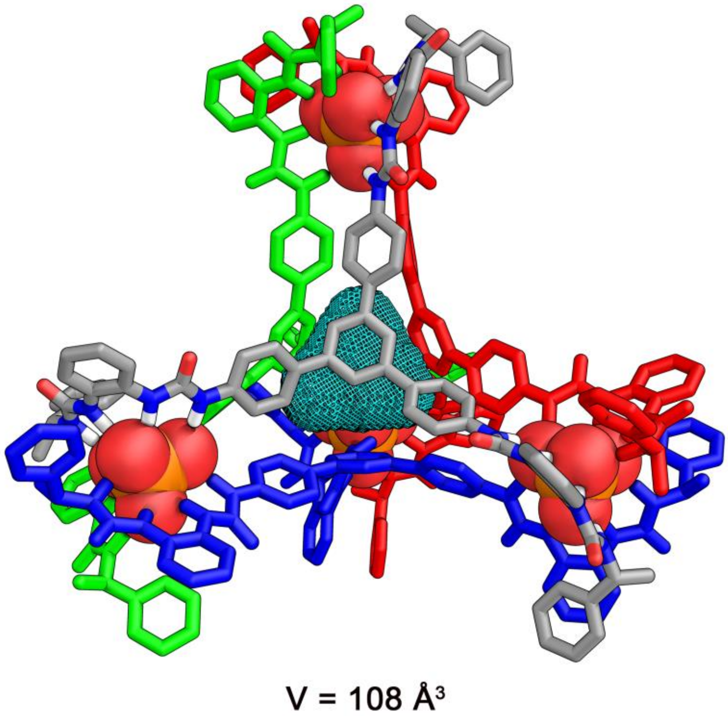

Figure S51. Cavity volume of **1^{R}**.

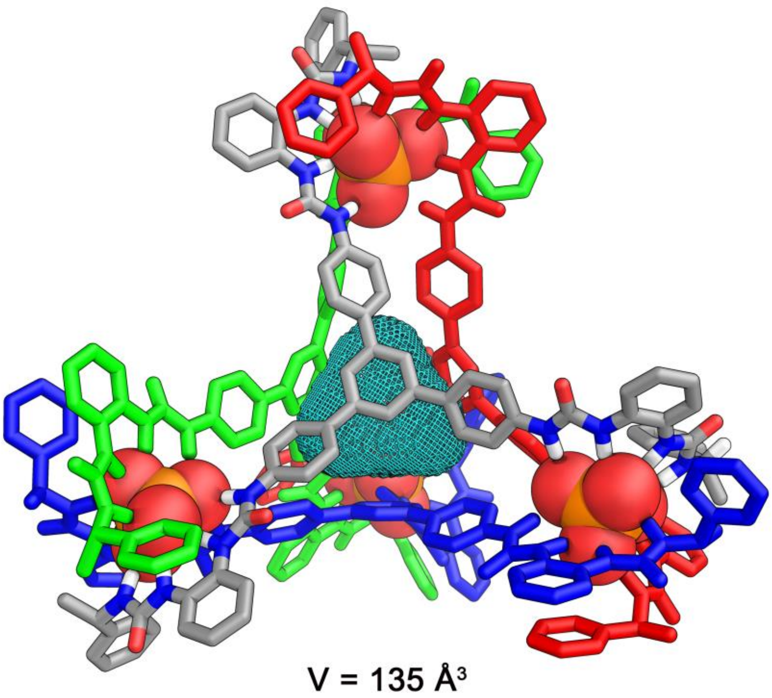

Figure S52. Cavity volume of **1^{S}.**

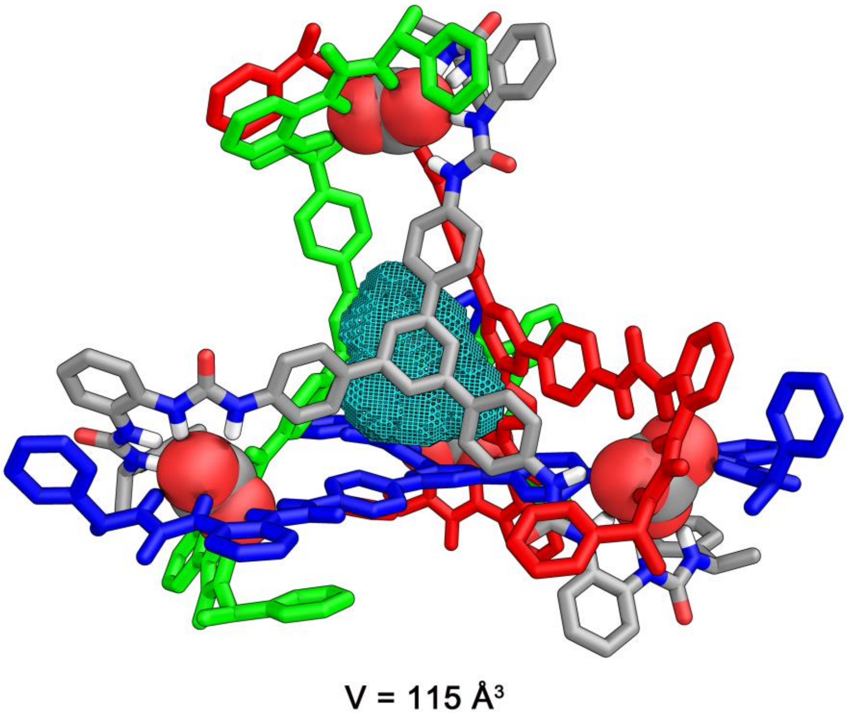

Figure S53. Cavity volume of **3**$^{\mathbf{R}}$.

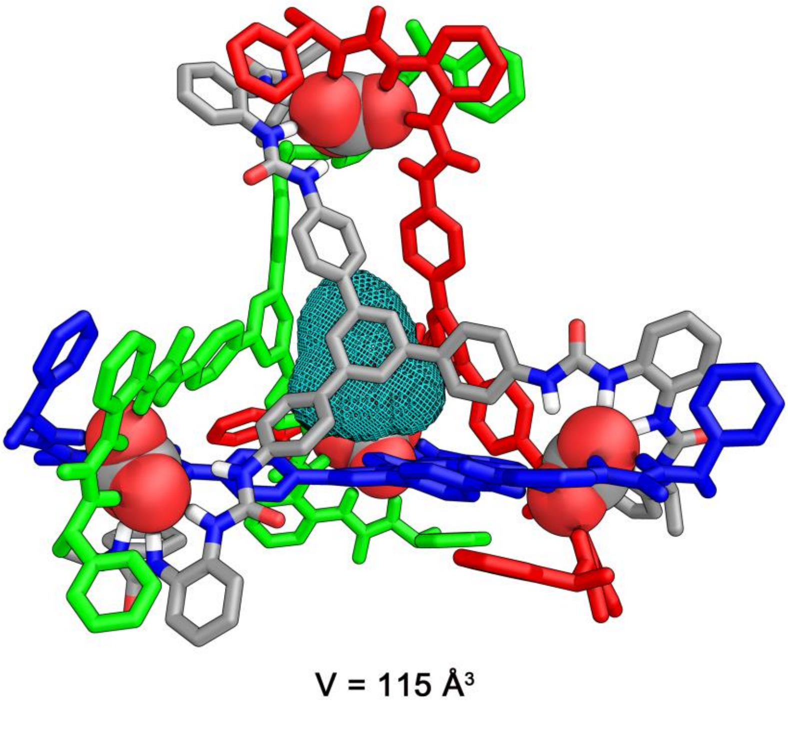

Figure S54. Cavity volume of **3**$^{\mathbf{S}}$.

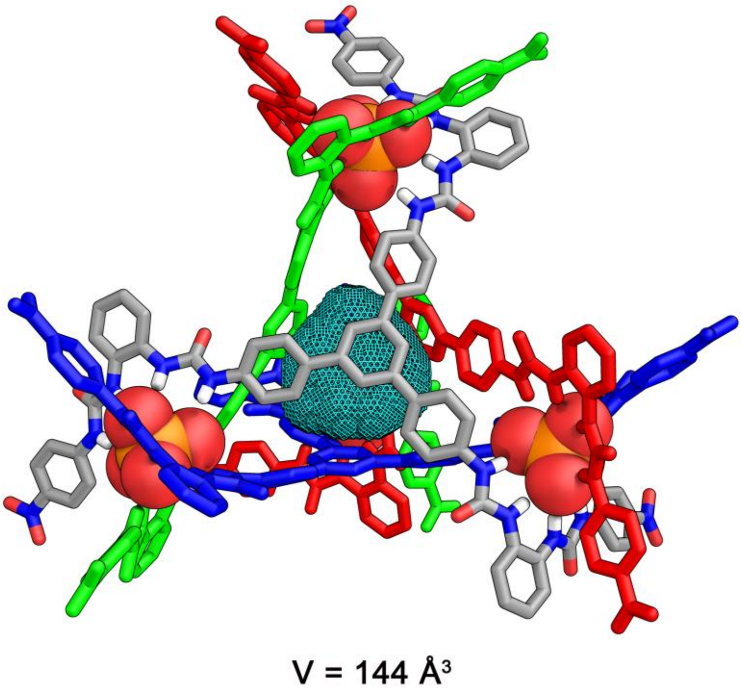

Figure S55. Cavity volume of the achiral tetrahedral cage ($\mathbf{L}^{\mathbf{NO2}}$ with PO_4^{3-}).

S7. Circular dichroism (CD) characterization

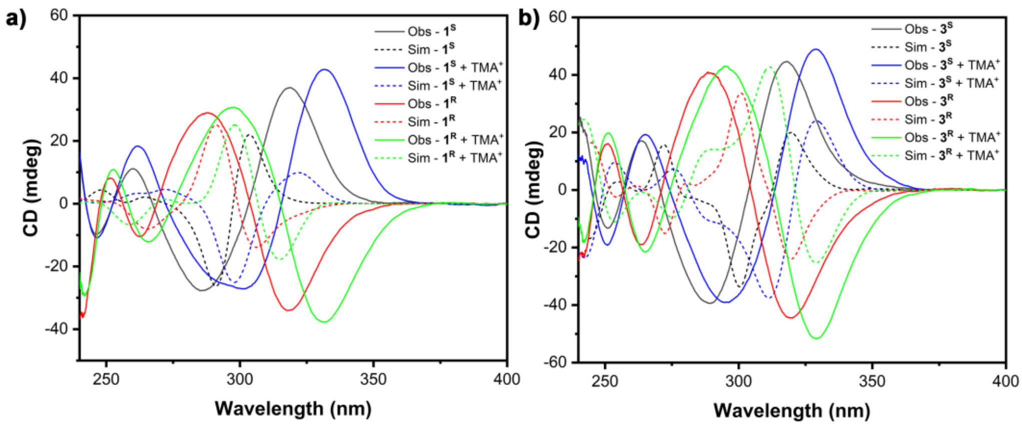

Figure S56. The CD spectra and theoretical calculation of CD spectra of a) $\mathbf{1}^{\mathbf{R/S}}$, $\mathbf{1}^{\mathbf{R/S}}$ with addition of TMA^+; b) $\mathbf{3}^{\mathbf{R/S}}$, and $\mathbf{3}^{\mathbf{R/S}}$ with addition of TMA^+.

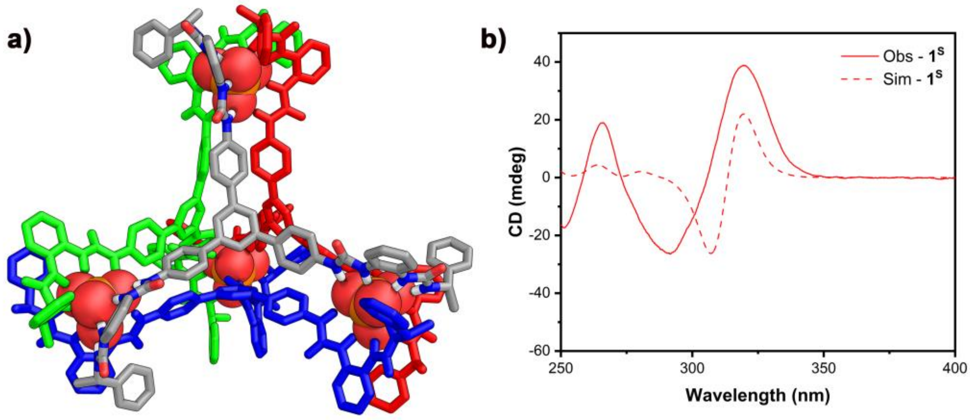

Figure S57. A) Molecular model of $\mathbf{1}^{\mathbf{S}}$. B) The CD spectra and theoretical calculation of CD spectra of $\mathbf{1}^{\mathbf{S}}$.

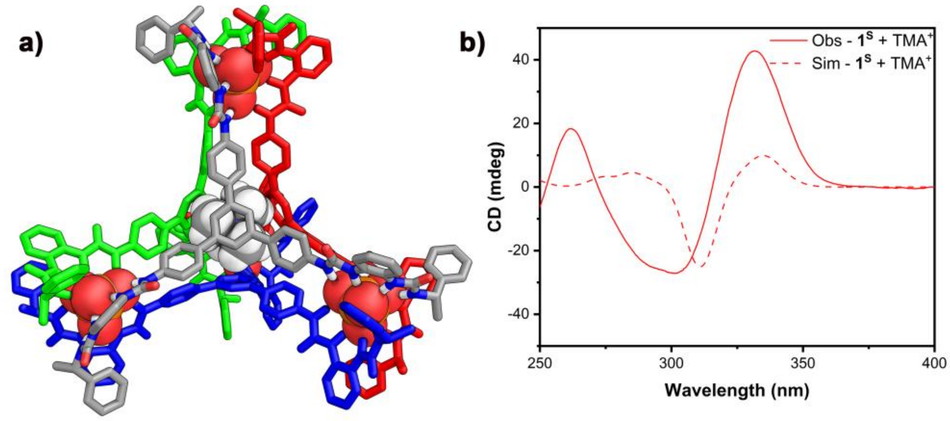

Figure S58. A) Molecular model of $\mathbf{1}^{\mathbf{S}}$ with encapsultion of TMA$^+$. B) The CD spectra and theoretical calculation of CD spectra of $\mathbf{1}^{\mathbf{S}}$ with addition of TMA$^+$.

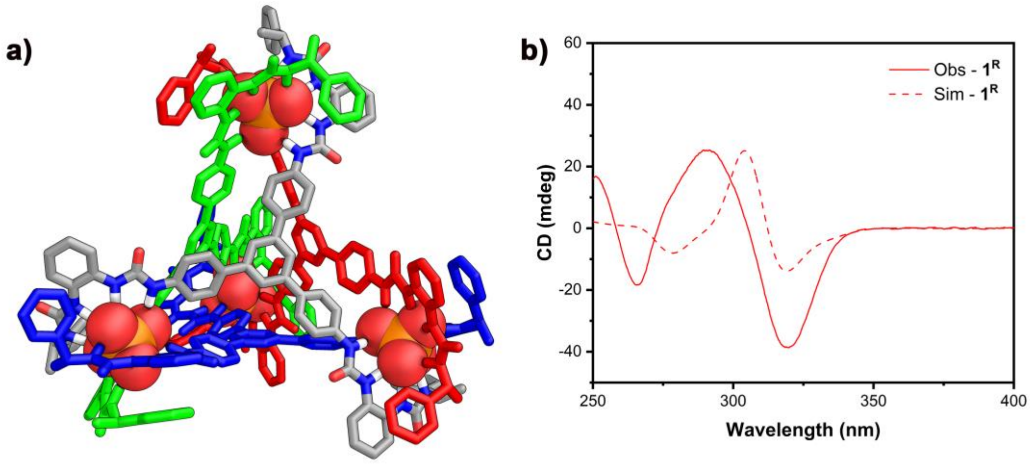

Figure S59. A) Molecular model of $\mathbf{1}^{\mathbf{R}}$. B) The CD spectra and theoretical calculation of CD spectra of $\mathbf{1}^{\mathbf{R}}$.

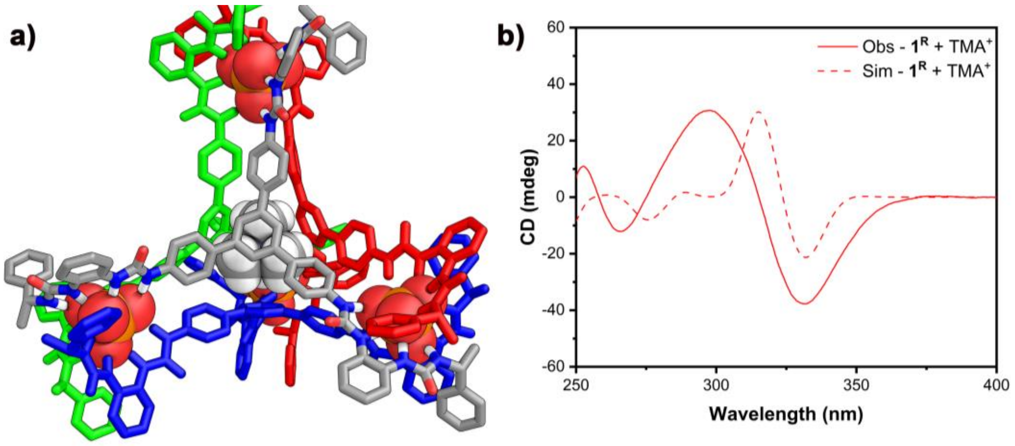

Figure S60. a) Molecular model of $\mathbf{1^R}$ with encapsultion of TMA^+. b) The CD spectra and theoretical calculation of CD spectra of $\mathbf{1^R}$ with addition of TMA^+.

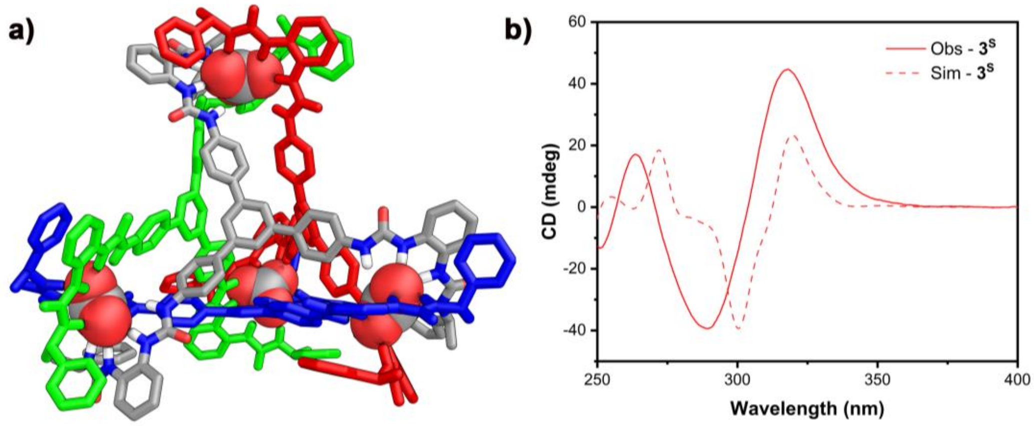

Figure S61. a) Molecular model of $\mathbf{3^S}$. b) The CD spectra and theoretical calculation of CD spectra of $\mathbf{3^S}$.

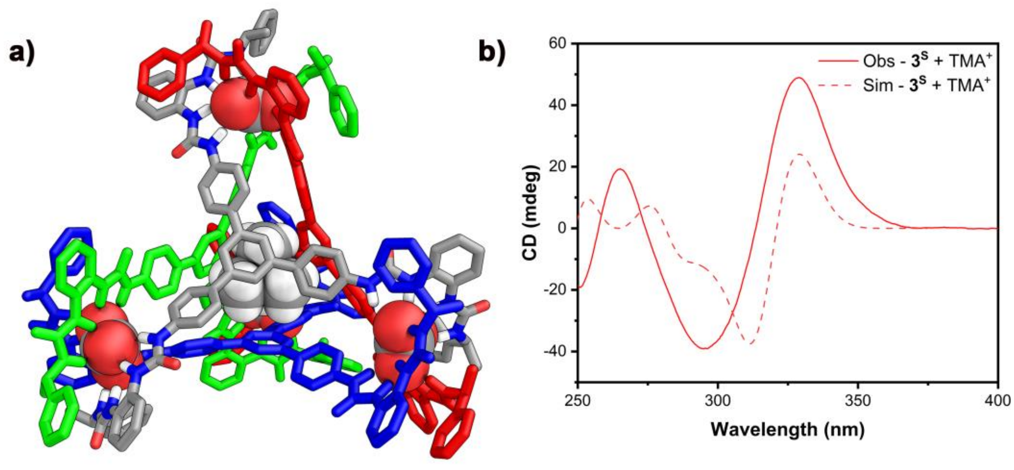

Figure S62. a) Molecular model of $\mathbf{3^S}$ with encapsultion of TMA^+. b) The CD spectra and theoretical calculation of CD spectra of $\mathbf{3^S}$ with addition of TMA^+.

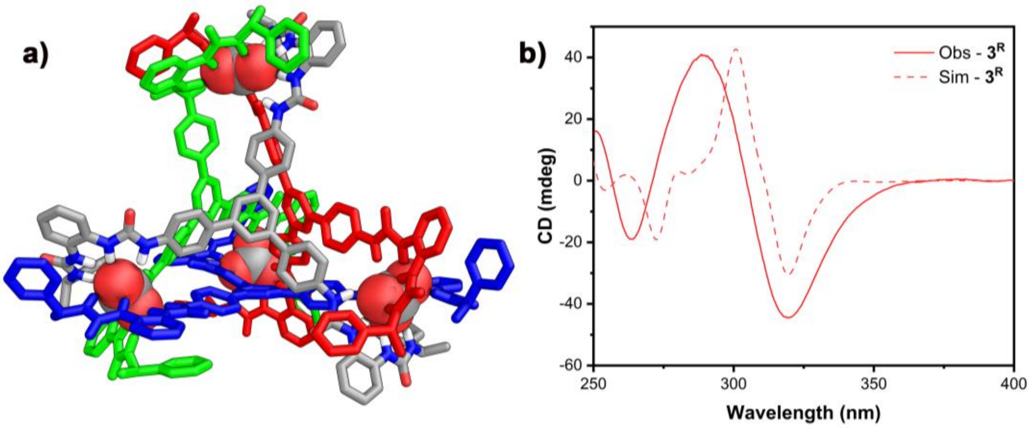

Figure S63. a) Molecular model of $\mathbf{3^R}$. b) The CD spectra and theoretical calculation of CD spectra of $\mathbf{3^R}$.

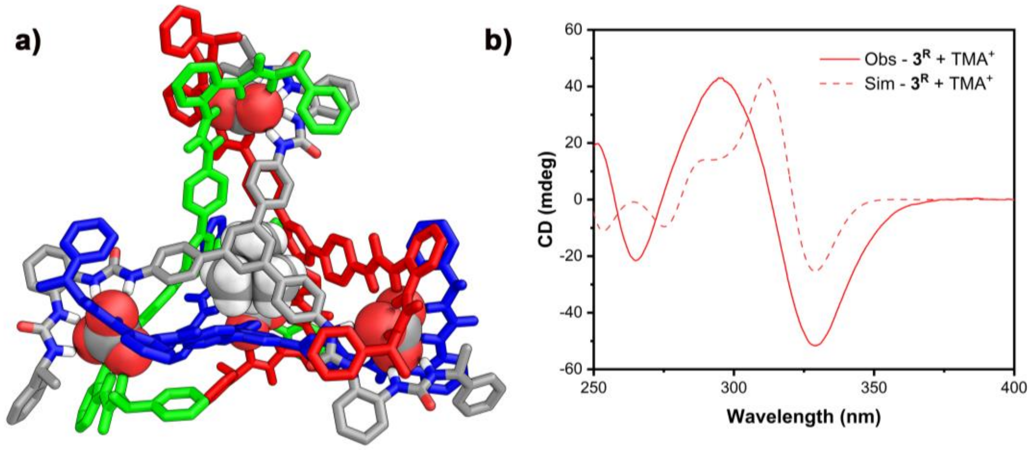

Figure S64. a) Molecular model of $\mathbf{3^R}$ with encapsultion of TMA$^+$. b) The CD spectra and theoretical calculation of CD spectra of $\mathbf{3^R}$ with addition of TMA$^+$.

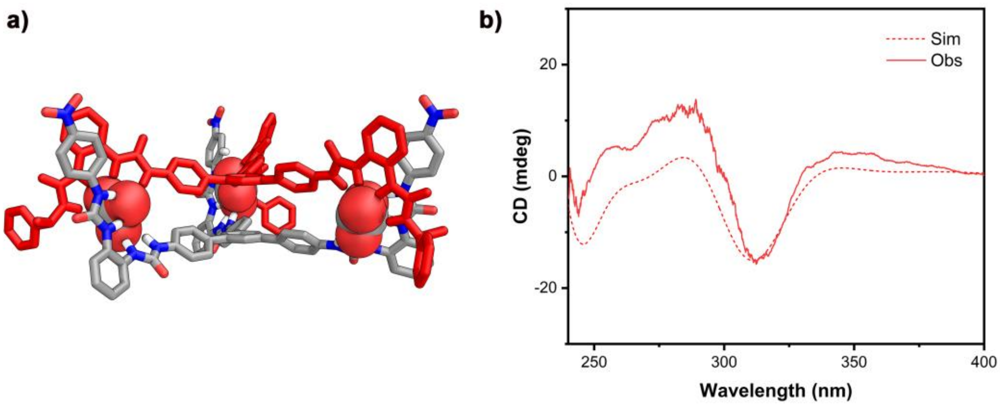

Figure S65. a) Molecular model of carbonate-coordinated mixed-ligand trinuclear pinwheel-like helical structure. b) The CD spectra and theoretical calculation of CD spectra of carbonate-coordinated mixed-ligand ($\mathbf{L^S}$: $\mathbf{L^{NO2}}$ = 1 : 3) structure.

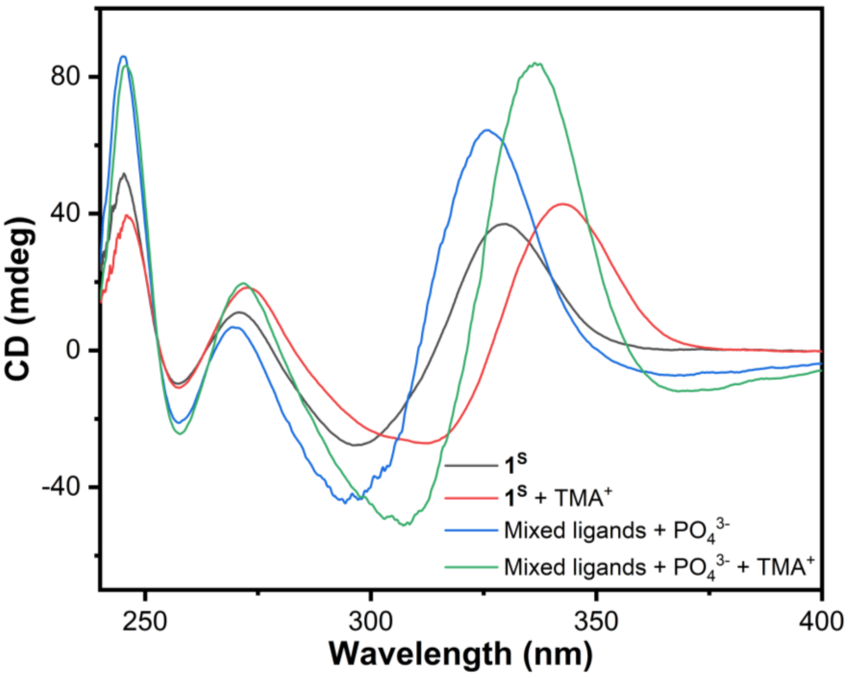

Figure S66. CD spectra of $\mathbf{1}^{\mathbf{S}}$, $\mathbf{1}^{\mathbf{S}}$ with addition of TMA^+, phosphate-coordinated mixed-ligand ($\mathbf{L}^{\mathbf{S}}$: $\mathbf{L}^{\mathbf{NO2}}$ = 1 : 3) cage (self-assembly with 10 eq. $[K(18\text{-}C\text{-}6)]_3PO_4$) and subsequent addition of 1 eq. TMACl.

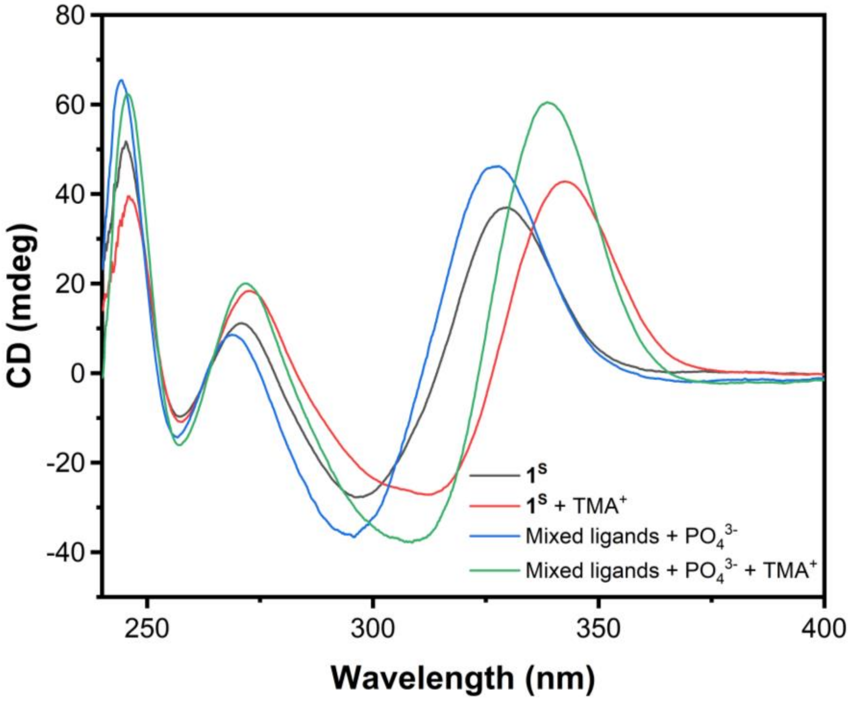

Figure S67. CD spectra of $\mathbf{1}^{\mathbf{S}}$, $\mathbf{1}^{\mathbf{S}}$ with addition of TMA^+, phosphate-coordinated mixed-ligand ($\mathbf{L}^{\mathbf{S}}$: $\mathbf{L}$ = 1 : 1) cage (self-assembly with 10 eq. $[K(18\text{-}C\text{-}6)]_3PO_4$), and subsequent addition of 1 eq. TMACl.

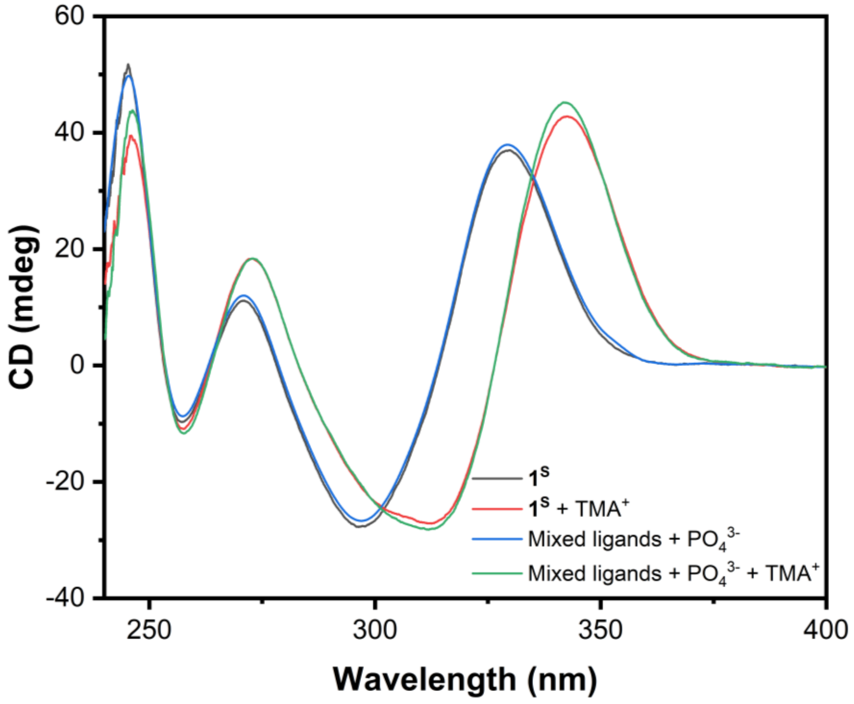

Figure S68. CD spectra of $\mathbf{1^S}$, $\mathbf{1^S}$ with addition of TMA^+, phosphate-coordinated mixed-ligand ($\mathbf{L^S}$: $\mathbf{L}$ = 3 : 1) cage (self-assembly with 10 eq. $[K(18\text{-}C\text{-}6)]_3PO_4$), and subsequent addition of 1 eq. TMACl.

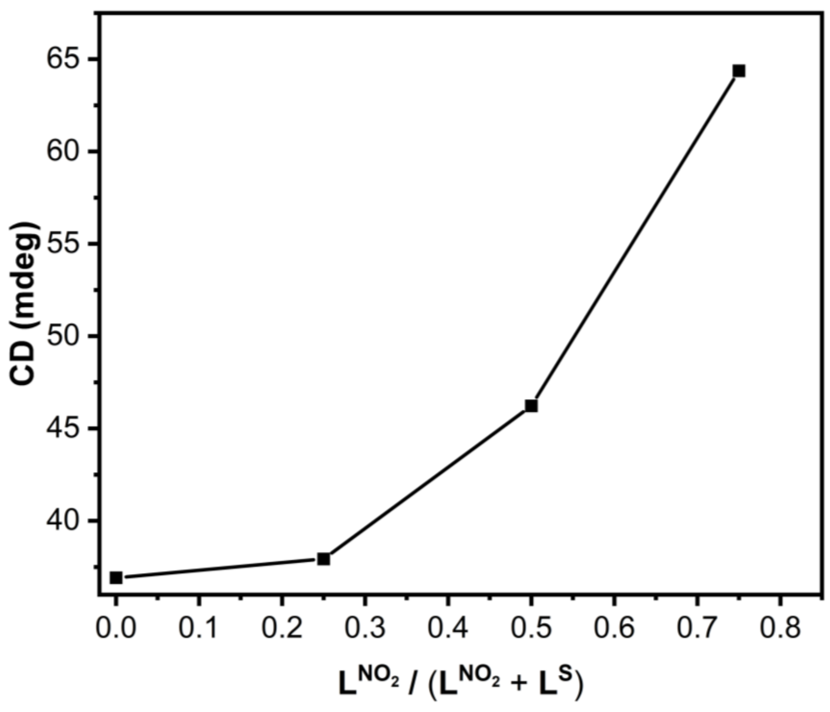

Figure S69. Plots of CD intensities (327 nm) of the tetrahedral cage $(PO_4)_4(\mathbf{L^{NO2}})_{4\text{-}n}(\mathbf{L^S})_n$ (n = 0−4) as a function of $\mathbf{L^{NO2}}$ proportion (keeping the concentration of $\mathbf{L^S}$ at 0.1 mM).

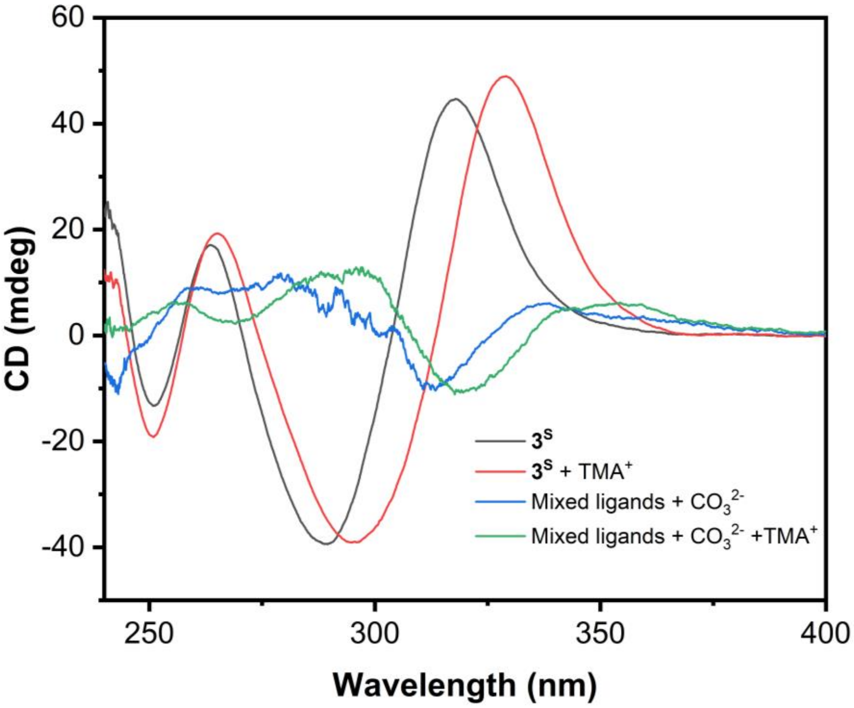

Figure S70. CD spectra of $\mathbf{3}^{\mathbf{S}}$, $\mathbf{3}^{\mathbf{S}}$ with addition of TMA^+, carbonate-coordinated mixed-ligand ($\mathbf{L}^{\mathbf{S}}$: $\mathbf{L}$ = 1 : 3) structure (self-assembly with 2 eq. $[K(18\text{-}C\text{-}6)]_2CO_3$), and subsequent addition of 1 eq. TMACl.

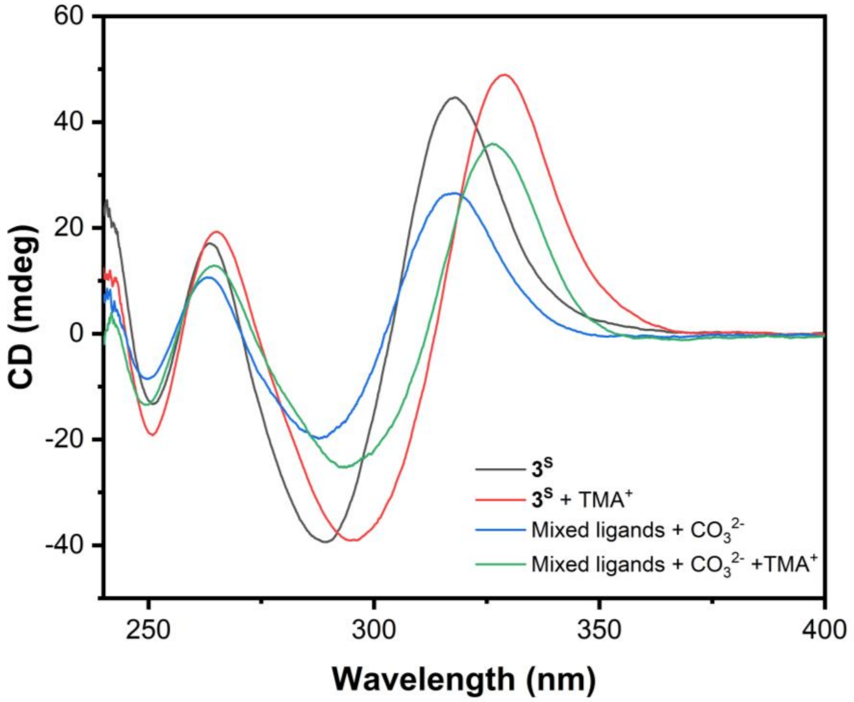

Figure S71. CD spectra of $\mathbf{3}^{\mathbf{S}}$, $\mathbf{3}^{\mathbf{S}}$ with addition of TMA^+, carbonate-coordinated mixed-ligand ($\mathbf{L}^{\mathbf{S}}$: $\mathbf{L}$ = 1 : 1) structure (self-assembly with 10 eq. $[K(18\text{-}C\text{-}6)]_2CO_3$), and subsequent addition of 1 eq. TMACl.

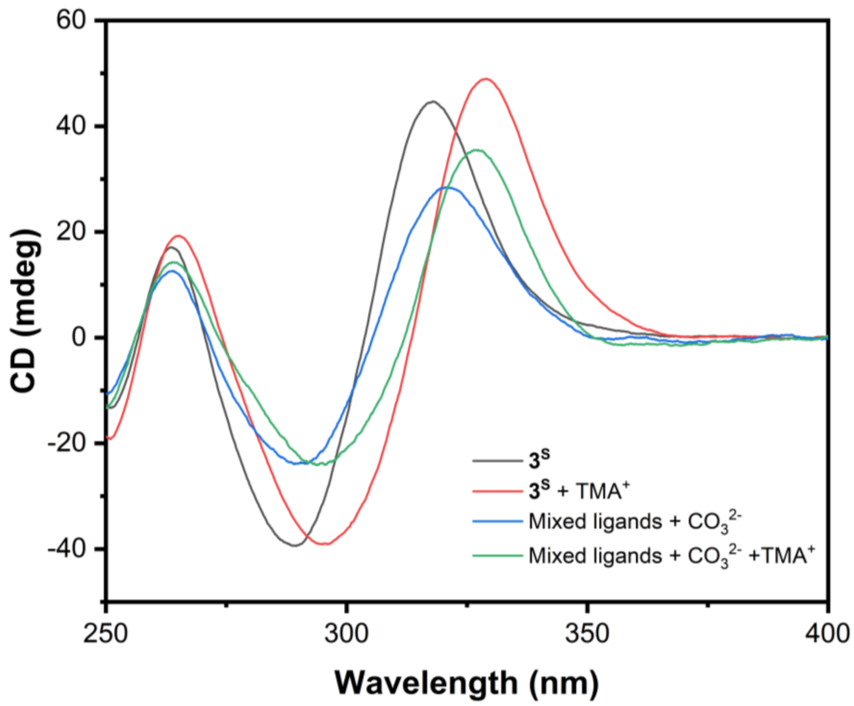

Figure S72. CD spectra of $\mathbf{3}^{\mathbf{S}}$, $\mathbf{3}^{\mathbf{S}}$ with addition of TMA^+, carbonate-coordinated mixed-ligand ($\mathbf{L}^{\mathbf{S}}$: $\mathbf{L}$ = 3 : 1) structure (self-assembly with 4 eq. $[K(18\text{-}C\text{-}6)]_2CO_3$), and subsequent addition of 1 eq. TMACl.

Reference

1. D. Yang, J. Zhao, Y. Zhao, Y. Lei, L. Cao, X.-J. Yang, M. Davi, N. Amadeu de Sousa, C. Janiak, Z. Zhang, Y.-Y. Wang and B. Wu, *Angew. Chem., Int. Ed.*, 2015, ***54***, 8658-8661.

2. C. Bannwarth, E. Caldeweyher, S. Ehlert, A. Hansen, P. Pracht, J. Seibert, S. Spicher and S. Grimme, *WIREs Comput Mol Sci.*, 2021, ***11***, e1493.

3. S. Grimme and C. Bannwarth, *J. Chem. Phys.*, 2016, ***145***, 054103.

4. R. L. J. B. Maglic, *J. Appl. Cryst.*, 2021, ***55***, 1033-1044.